Journal Pre-proof

Inhibitor design to target a unique feature in the folate pocket of *Staphylococcus aureus* dihydrofolate reductase

N. Prasad Muddala, John C. White, Baskar Nammalwar, Ian Pratt, Leonard M. Thomas, Richard A. Bunce, K. Darrell Berlin, Christina R. Bourne

PII: S0223-5234(20)30383-4

DOI: https://doi.org/10.1016/j.ejmech.2020.112412

Reference: EJMECH 112412

To appear in: *European Journal of Medicinal Chemistry*

Received Date: 24 February 2020

Revised Date: 28 April 2020

Accepted Date: 28 April 2020

Please cite this article as: N.P. Muddala, J.C. White, B. Nammalwar, I. Pratt, L.M. Thomas, R.A. Bunce, K.D. Berlin, C.R. Bourne, Inhibitor design to target a unique feature in the folate pocket of *Staphylococcus aureus* dihydrofolate reductase, *European Journal of Medicinal Chemistry* (2020), doi: https://doi.org/10.1016/j.ejmech.2020.112412.

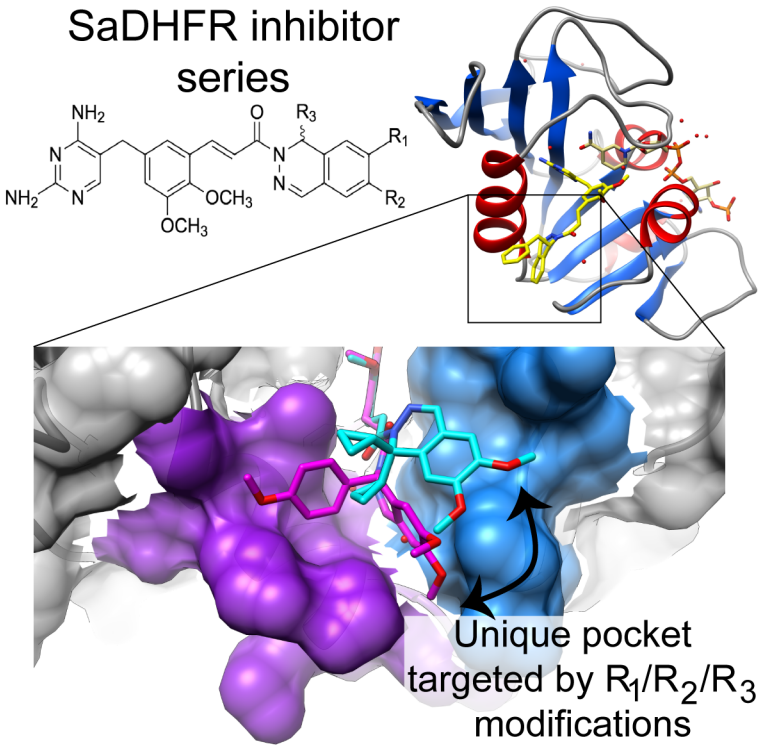

Inhibitor design to target a unique feature in the folate pocket of *Staphylococcus aureus* dihydrofolate reductase

N. Prasad Muddala[1,¶,#a], John C. White[2,¶], Baskar Nammalwar[1,#b], Ian Pratt[2], Leonard M. Thomas[2], Richard A. Bunce[1], K. Darrell Berlin[1], and Christina R. Bourne[2*]

1: Department of Chemistry, 107 Physical Sciences I, Oklahoma State University, Stillwater, OK 74078

2: Department of Chemistry and Biochemistry, 101 Stephenson Parkway, University of Oklahoma, Norman, OK 73019

[¶]Co-first authors with equivalent contributions, order determined alphabetically

*Corresponding author: cbourne@ou.edu +1 (405) 325-5348

[#a]Current Address: Impec Labs, Plot No. 5-5-35/87/1, 401, Prasanthi Nagar, IDA Kukatpally, Hyderabad-500072, India

[#b]Current Address: Forge Therapeutics, 10578 Science Center Drive, Suite 205, San Diego, California-92121, USA

Running Title: Targeting SaDHFR inhibitors to a unique surface pocket

Keywords: Dihydrofolate reductase, 2,4-diaminopyrimidine, *Staphylococcal aureus*, antibacterial, enzyme inhibition, folate pathway, Heck coupling, alkyl dihydrophthalazines

Abstract

Staphylococcus aureus (Sa) is a serious concern due to increasing resistance to antibiotics. The bacterial dihydrofolate reductase enzyme is effectively inhibited by trimethoprim, a compound with antibacterial activity. Previously, we reported a trimethoprim derivative containing an acryloyl linker and a dihydophthalazine moiety demonstrating increased potency against *S. aureus*. We have expanded this series and assessed *in vitro* enzyme inhibition (K_i) and whole cell growth inhibition properties (MIC). Modifications were focused at a chiral carbon within the phthalazine heterocycle, as well as simultaneous modification at positions on the dihydrophthalazine. MIC values increased from 0.0626 – 0.5 µg/mL to the 0.5 – 1 µg/mL range when the edge positions were modified with methyl or methoxy groups. Changes at the chiral carbon affected K_i measurements but with little impact on MIC values. Our structural data revealed accommodation by only the *S*-enantiomer of the inhibitors within the folate-binding pocket. Longer modifications at the chiral carbon, such as *p*-methylbenzyl, would protrude from the pocket into solvent and result in poorer K_i values, as do modifications with greater torsional freedom, such as 1-ethylpropyl. The most efficacious K_i was 0.7 ± 0.3 nM, obtained with a cyclopropyl derivative containing dimethoxy modifications at the dihydrophthalazine edge. The co-crystal structure revealed an alternative placement of the phthalazine moiety into a shallow surface at the edge of the site that can accommodate either enantiomer of the inhibitor. The current design, therefore, highlights how to engineer specific placement of the inhibitor within this alternative pocket, which in turn maximizes the enzyme inhibitory properties.

1. Introduction

The emergence of antibiotic resistance negatively impacts human life and causes a substantial financial burden to society [1, 2]. *Staphylococcus aureus,* a gram-positive pathogen, contributes substantially to serious human infections. Recent increases in *S. aureus* infections have resulted from both a rise in nosocomial cases, including endocarditis and growth on implanted devices, as well as through an increased prevalence of skin and soft tissue infections. A recent study utilized whole genome sequencing methods to track public exposure to pathogens and discovered high levels of drug-resistant *S. aureus* in public spaces [3]. In 2017, the Centers for Disease Control reported that 119,000 people in the US suffered from bloodstream infections caused by both drug resistant and sensitive strains of this organism; of these, 20,000 individuals succumbed to the infection [4]. Furthermore, a sharp spike in *S. aureus* infections has been associated with increased intravenous opioid abuse (4). Overall, this highlights the continuing need for control measures to combat *S. aureus* infections.

The bacterial biosynthetic folate pathway has provided important strategic advances for controlling bacterial growth, for which the synthetic compound trimethoprim (TMP) is a gold standard inhibitor [5]. Mutations conferring resistance to trimethoprim are partially responsible for the increased treatment failures of *S. aureus* infections [6-8], as are additional mobile isoforms of DHFR containing mutations rendering them less susceptible to TMP [9]. The folate pathway is also of interest due to the unusual synergy of TMP-inhibited dihydrofolate reductase (DHFR) enzyme when combined with one of the sulfa drug classes that inhibit the dihydroneopterin synthase enzyme. The cause of this unique and highly potent synergy has recently been defined as “mutual potentiation” that arises from stagnated metabolic flux of the precursor substrates [10]. Given the many positive benefits from DHFR inhibition, the development of next generation antifolates continues to be heavily pursued [11, 12].

Inhibitors of DHFR are typically substrate mimetics that mediate competitive inhibition with respect to the dihydrofolate. While these have wide medical applications targeting mammalian DHFR [for example, 13-15], the current work is focused on compounds

specific for bacterial versions of DHFR. Considered “non-classical” due to the lack of glutamylation, many rely on replacement of the native pterin heterocycle with a 2,4-diaminopyrimidine (DAP) ring [11, 12, 16, 17]. One such highly potent DAP-containing DHFR inhibitor is Iclaprim, originally developed by Basilea Pharmaceutica (Switzerland). Despite multiple clinical trials and FDA applications for treatment of acute bacterial skin and skin structure infections and hospital acquired bacterial pneumonia, it is currently no longer in development [18, 19]. These reports indicate levels of hepatotoxicity, although the extent of this is unclear. Other successful DAP-containing DHFR inhibitors include a collection of 7-aryl-2,4-diaminoquinazolines, in particular Rx101005, developed by Trius Therapeutics and recently acquired by Merck *via* Cubist Pharmaceuticals (San Diego, CA). This compound has potent *in vivo* anti-*Staphylococcal* activity and is highly bioavailable, but its development has been discontinued [20]. A similar result was obtained for AR-709, which was developed by Evolva (Switzerland) but is no longer listed as an active project [21, 22]. Another compound, Emmacin, was identified through a diversity synthesis project sponsored by AstraZeneca and Pfizer and is highly potent for MRSA; its current status is unknown [23]. There is on-going active development of propargyl-linked trimethoprim derivatives that have demonstrated potent activity against a wide spectrum of MRSA isolates [9, 24]. For this series, the linker extending beyond the DAP ring is longer and rigid, allowing the compounds to explore unique positions within the main folate pocket that impact the co-factor NADPH placement.

The series of inhibitors in the current work were derived from compounds originally designed by Basilea that led to the development of Iclaprim. Our earlier studies demonstrated potent MIC values (≤ 0.0625-0.125 ug/mL) for MRSA and VRSA, which are approximately 64-times more potent than the standard of care TMP-sulfa drug combination [6]. These inhibitor molecules are based on trimethoprim, but are extended from the central dimethoxyphenyl ring *via* an acryloyl linker with an appended dihydrophthalazine system. The acryloyl linker allows rotational freedom of the phthalazine moiety relative to the remaining 2,4-diaminopyrimidine (DAP) trimethoprim-like structure. Structure determinations confirmed the exquisite conformational fit of the

dihydrophthalazine ring system to the distal portion of the DHFR binding site from *S. aureus,* as well as *B. anthracis* and *E. faecalis* [6, 25, 26]. These studies revealed an unusual plasticity in the *S. aureus* DHFR site, delineated by the dihydrophthalazine docked both in the canonical deeper folate binding pocket, as well as on a more surface-exposed shallow cavity at the distal portion of the binding site [6].

2. Results and discussion

2.1 Design of the novel *Staphylococcus aureus* dihydrofolate reductase inhibitors

To further explore this phenomenon, we have now tested additional derivatives that vary at the chiral center of the dihydrophthalazine, and in addition, have characterized the impact of derivatization of the distal phthalazine edge with methyl or methoxy groups. The moieties at the dihydrophthalazine chiral center have subtle influences on inhibition, such that as they extend in length from the dihydrophthalazine, the inhibition in general is reduced. This is likely due to surface exposure as they protrude outward from the folate pocket. However, additional space occupied laterally along the binding site by such modifications is favored, possibly due to additional contacts along the rim of the binding pocket. Interestingly, derivatization of C6 and C7 of the dihydrophthalazine with OCH_3 or CH_3 greatly impacted the whole cell inhibition (MIC values). This may be due to a more limited ability to diffuse across cell membranes and thus interact with the DHFR target. In general, completed crystal structures support these findings. Surprisingly, however, one derivative was able to completely occupy the shallow surface pocket unique to *S. aureus* DHFR. This inhibitor structure combined a smaller cyclopropyl at the chiral center of the dihydrophthalazine and bulkier methoxy additions at the dihydrophthalazine edge. It remains to be seen if this inhibitor would interact and inhibit other DHFR enzymes from bacteria that do not have this shallow surface. Additional structures provide insights on the hydration of the empty folate-binding pocket, with highly ordered and conserved water molecules demarking the polar interaction sites with inhibitors. Further optimizing interactions at these polar sites would provide additional improvement of inhibitors. The current inhibitor design clearly outlines how to manipulate occupancy of the traditional deeper folate-binding pocket versus the shallower surface pocket unique to *S. aureus*.

2.2 Chemistry

Compounds were varied at the chiral stereocenter (**Fig. 1**, "R_3" and Table S1), as this position was previously identified as impacting the inhibitory profile of other bacterial DHFR enzymes [25, 26]. Additional new modifications of methyl or methoxy substituents at the distal positions of the dihydrophthalazine moiety were also explored (**Fig. 1**, "R_1, R_2"). A series of racemic compounds was synthesized as shown in Scheme I. The structural motif of these desired targets was achieved by synthesizing two separate ring systems: the (i) 2,4-diaminopyrimidine ring (Scheme I) and the (ii) substituted dihydrophthalazine rings (Scheme II).

The 2,4-diaminopyrimidine ring was generated from 5-iodovanillin derivative **2**, as previously described [27]. The 2,4-diaminopyrimidine ring construction involved the preparation of 3-morpholinopropionitirile (**1**) reacting with **2** and NaOEt using DMSO as solvent to obtain an adduct that later underwent cyclization in the presence of $PhNH_2$.HCl, guanidine hydrochloride and NaOEt in EtOH, to achieve the desired **3** as shown in Scheme I.

Scheme I

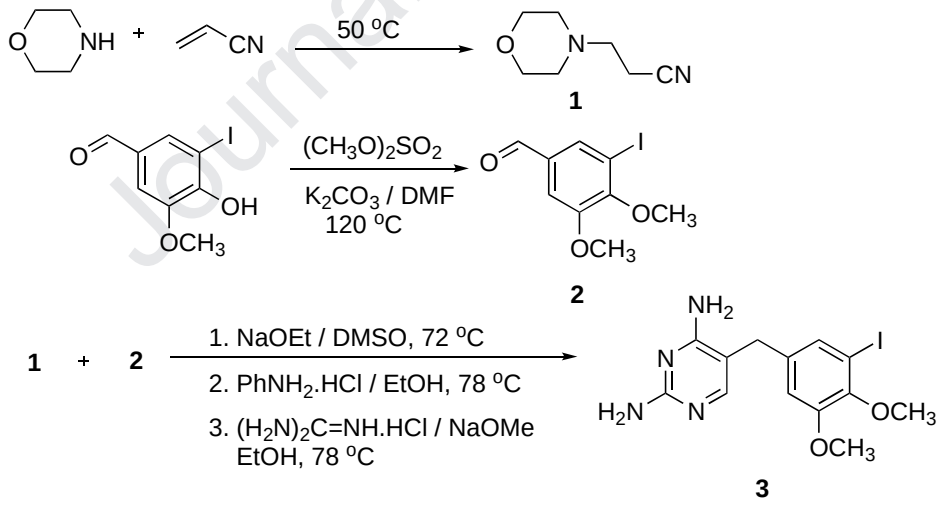

The phthalazine moieties for the desired targets were obtained commercially or by constructing substituted phthalazine heterocycles using a previously published procedure.[28, 29] These substituted phthalazines (**4** and **5**) were subjected to treatment with organomagnesium reagents in THF under anhydrous conditions to provide racemic intermediates (**7** and **8**) in Scheme II. These intermediates were further

subjected to *N*-acylation using acryloyl chloride and triethylamine in DCM to obtain the H/methyl/methoxy 1,2-dihydrophthalazine derivatives (**9** and **10**). Coupling of the acrylamides **9** and **10** with 2,4-diaminopyrimidine derivatives **3** was achieved *via* a Heck reaction in the presence of $Pd(OAc)_2$ and *N*-ethylpiperidine to afford the desired drug candidates (**12** and **13**) in yields of 80-90% as shown in Scheme II [28-30].

Scheme II

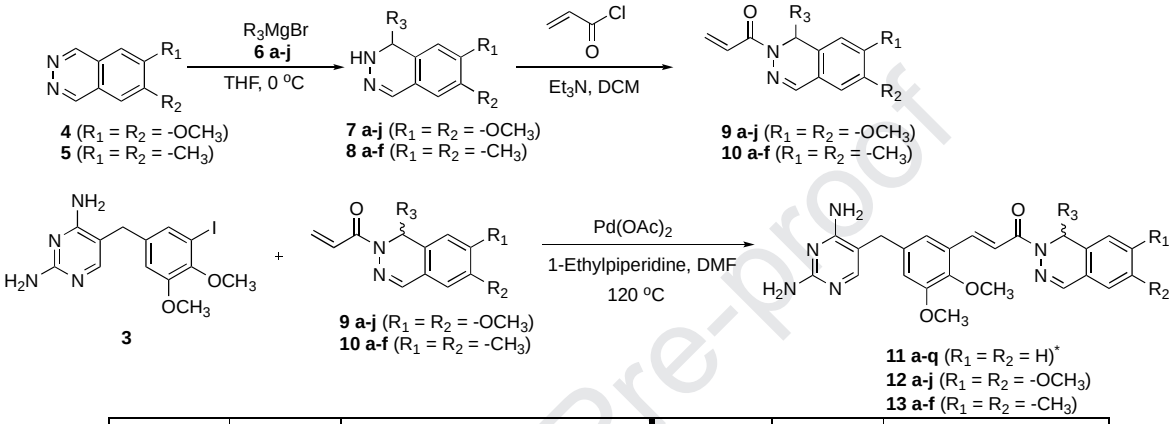

Inhibitor Name	$R_1 = R_2$	R_3	Inhibitor Name	$R_1 = R_2$	R_3
11a*	H	propyl	**12a**	$-OCH_3$	ethyl
11b*	H	isopropyl	**12b**	$-OCH_3$	propyl
11c*	H	trifluoropropyl	**12c**	$-OCH_3$	cyclopropyl
11d*	H	isobutyl	**12d**	$-OCH_3$	vinyl
11e*	H	isobutenyl	**12e**	$-OCH_3$	isobutenyl
11f*	H	1-ethylpropyl	**12f**	$-OCH_3$	phenyl
11g*	H	cyclohexyl	**12g**	$-OCH_3$	*o*-tolyl
11h*	H	phenyl	**12h**	$-OCH_3$	*o*-ethylphenyl
11i*	H	*o*-tolyl	**12i**	$-OCH_3$	*o*-methoxyphenyl
11j*	H	*p*-tolyl	**12j**	$-OCH_3$	*p*-methoxyphenyl
11k*	H	3,5-dimethylphenyl	**13a**	$-CH_3$	ethyl
11l*	H	*m*-fluorophenyl	**13b**	$-CH_3$	propyl
11m*	H	*p*-fluorophenyl	**13c**	$-CH_3$	cyclopropyl
11n*	H	benzyl	**13d**	$-CH_3$	vinyl
11o*	H	*p*-methylbenzyl	**13e**	$-CH_3$	isobutenyl
11p*	H	*p*-methoxybenzyl	**13f**	$-CH_3$	phenyl
11q*	H	*p*-trifluoromethoxybenzyl			

* The synthesis of **11a-q** is reported in our previous publication[24]

3. Biological evaluation

3.1 Efficacy of inhibitors with SaDHFR enzyme activity and *S. aureus* growth

The potency of each compound was evaluated for *in vitro* inhibition of the target DHFR enzyme, and cell-based for its ability to prevent the growth of *S. aureus* cultures. In general, trends of potency were correlated in both these assays. For ease of interpretation, the compounds are grouped based on the properties of the modifications at position R_3.

The group of alkyl-based modifications at R_3 included ethyl, propyl, isopropyl, cyclohexyl, trifluoropropyl, isobutyl, isobutenyl, cyclopropyl, vinyl, and 1-ethylpropyl (**Fig. 1**). The most efficacious modifications for *in vitro* enzyme inhibition were the cyclohexyl (**11g**) and cyclopropyl (**12c**) moieties, followed by isopropyl (**11b**), propyl (**11a**), and trifluoropropyl (**11c**), and with only slightly less potency when isobutyl (**11d**) or isobutenyl (**11e**) were installed. This is a distinctly different preference profile from that of *B. anthracis* DHFR, where the isobutyl and isobutenyl modifications were equally the most potent [31]. Finally, 1-ethylpropyl (**11f**) installed at R_3 was the least effective at mediating enzyme inhibition among this series. When the torsional freedom of this group is compared to, for example, the most potent inhibitor with a cyclohexyl moiety (**11g**), it is clear that restricting the torsional freedom of the moiety at this position results in better inhibition. When tested for whole cell inhibition of *S. aureus* cell growth, variations in compound potency become less obvious (**Fig. 1**). However, dihydrophthalazine derivatization at R_1 and R_2 negatively impacts the MIC values by 2- to 4-times, with the dimethoxy modification producing the least favorable inhibition. For example, when R_3 = propyl, the K_i values resulting from enzyme inhibition are essentially the same, regardless of the dihydrophthalazine ring modification (1.2 ± 0.1 nM with $R_1 = R_2 = H$ (**11a**), 1.1 ± 0.7 nM with $R_1 = R_2 = OCH_3$ (**12b**), and 1.2 ± 0.5 nM with $R_1 = R_2 = CH_3$ (**13b**)). However, the MIC values are 0.0625-0.25 μg/mL for $R_1 = R_2 = H$ (**11a**), 1 μg/mL for $R_1 = R_2 = OCH_3$ (**12b**), and 0.5-1 μg/mL for $R_1 = R_2 = CH_3$ (**13b**). Overall, this trend is consistently independent of the modification at the R_3 position, indicating that the changes in potency must be due to solubility and membrane permeability of these derivatives rather than direct inhibition at the target enzyme.

The exception to this trend is the compound with $R_1 = R_2 = OCH_3$ and R_3 = cyclopropyl (**12c**). It is strikingly potent *in vitro*, with the lowest K_i value at 0.7 ± 0.3 nM. The reason for this improved target inhibition became clear when structural studies were completed (below). However, this marked improvement was not realized at the whole cell level, with MIC values remaining at the highest value for this series at 1 µg/mL.

The next class of R_3 derivatives contains an aromatic moiety, and positions around this ring were modified. These modifications were extended to also assess hydrophobic versus polar substitutions. Overall, the placement of an aromatic moiety at position R_3 resulted in a very potent inhibitor. While the unsubstituted phenyl modification was among the most efficacious *in vitro*, modifications appending a methyl group in the *orthro,* or fluorine in the *para or meta* positions had essentially no impact on the K_i value. Alteration of the *para* position with methyl or dimethyl groups placed in equivalent *meta* positions had worse inhibition *in vitro*. However, the *p*-methyl addition (**11j**) had a surprisingly low MIC value, at 0.046-0.187 µg/mL. This was equivalent to the other lowest MIC value (0.938-0.1875 µg/mL) in this series (**11b,** R_3 = isopropyl). The trend of equivalent K_i values, and yet increasing MIC values with dihydrophthalazine derivatization at $R_1 = R_2$, is also evident with R_3 = aromatic moieties.

The final class of modifications was based on the success of aromatic substituents, but extended the length of the R_3 dihydrophthalazine heterocycle by one carbon atom, generating R_3 = benzyl derivatives (**11n-q**). This series is among the least effective, and so was not included in the $R_1 = R_2$ derivatization. Extension from the ring structure in the *para* position revealed a preference for a more polar *p*-methoxybenzyl group (**11p**, K_i 1.2 ± 0.4) in comparison to a nonpolar *p*-methylbenzyl moiety (**11o**, K_i 2.3 ± 0.4 nM), which was the least potent *in vitro* among all the tested compounds. This class appears to delineate the limit to modifications at this position, likely due to impinging on the protein:solvent boundary as the R_3 modifications become longer. This is also reflected in the whole cell phenotypic assay, where the MIC value range is intermediate with values of 0.25-1 µg/mL.

3.2 Binding poses of selected inhibitors in the folate pocket of SaDHFR

To assist in rationalizing results with this inhibitor series, we carried out crystallographic studies of SaDHFR co-crystallized with the co-factor NADPH and saturated with racemic inhibitor compounds (crystallographic data statistics are given in **Table S2**). These efforts resulted in complexed structures for four inhibitors with R_1 = R_2 = H, where R_3 was 1-ethylpropyl (**11f**), *p*-tolyl (**11j**), 3,5-dimethylphenyl (**11k**) and benzyl (**11n**), and two with R_1 = R_2 = OCH_3, where R_3 was cyclopropyl (**12c**) and *p*-methoxyphenyl (**12j**). In an attempted X-ray structure determination with R_1 = R_2 = H and R_3 = *p*-methoxybenzyl (**11p**), the folate pocket was discovered to be void of the inhibitor. This provided a fortuitous opportunity to compare the hydration of the empty folate pocket with those systems with the inhibitor-complexed structures.

The structure of the diaminopyrimidine (DAP) ring in the current inhibitor series is conserved from the compound trimethoprim, as are the contacting residues (**Fig. 2**) [32]. In particular, this portion of the binding site requires specific hydrogen bonds formed with substrate, with inhibitor, or with water molecules. An acidic residue at position 27 (Asp in Sa) forms hydrogen bonds to nitrogen atoms in the pterin of dihydrofolate or in the diaminopyrimidine of an inhibitor. There are additional hydrogen bonds between this amino moiety and the side chain oxygen of Thr111, as well as the main chain carbonyls of Leu5, Val6, and Phe92. The absence of an inhibitor in one of the crystal structures allows examination of the hydration of the folate pocket under these crystallization conditions. Multiple water molecules bind within the empty folate pocket and maintain a network that must be disrupted to allow substrate or inhibitor access. Specific waters are positioned to satisfy polar interactions previously noted to be critical to pterin or DAP binding (25,28). This pattern is extended by placement of a water molecule at the central face, and thus between the nitrogen atoms of the pyrimidine ring, which are typical of trimethoprim-based inhibitors and serve as a mimetic of the substrate nitrogen-containing dihydropteridin heterocycle. Other hydrogen bonds and interactions conserved in this area of the binding site are directed at the tetrahydropteridin-derived nitrogen that is reduced in the catalytic cycle. This nitrogen atom can form bonds with the main chain carbonyl oxygen of residue Phe92, as well as with atoms in the NADPH co-factor. Elemental analyses of the final

compounds **12a-j** and **13a-f** revealed a strong tendency to retain water, perhaps mimicking the polar interactions of the DAP ring within the DHFR folate pocket.

The only other polar interaction between SaDHFR and the inhibitors was between a methoxy group extending from the central ring, analogous to that found in trimethoprim, with the side chain of Ser49 (**Fig. 2B**). The remaining contacts are all hydrophobic, and as was previously noted, rely on shape complementarity to interact with the inhibitors [6, 30]. The closest approach of the inhibitor to atoms of the protein are carbon-carbon atoms in the 3.5 Å to 4 Å range of residues Leu28 and Leu54, with Phe92 protruding upwards from the base of the binding site and forming a surface that supports the acryloyl linker. The dihydrophthalazine heterocycle occupies a groove along the protein's substrate pocket and makes van der Waals contact and hydrophobic interactions with small hydrophobic residues or the aliphatic portions of longer side chain residues. In particular, amino acids Leu28, Lys29, Val31, Lys32, Leu54 and Pro55 line the crevice that conforms to the inhibitor shape (**Fig. 2B, C**). The aromatic portion of the dihydrophthalazine moiety is adjacent to the polar regions of side chains Asn56 and Arg57. The latter is a source of a persistently strained steric clash in all inhibitor-bound structures from these series.

Co-crystals with inhibitors containing R_3 = 1-ethylpropyl (**11f**, orange), *p*-tolyl (**11j**, light green), 3,5-dimethylphenyl (**12k**, teal), and benzyl (**11n**, yellow) variations revealed a remarkably conserved fit to the SaDHFR binding site (**Fig. 2C**). Each of these compounds contain predominantly the *S*-enantiomer, with minimal *R*-form visible for 1-ethylpropyl and *p*-tolyl derivatives. Given the low occupancy of these systems, they are not modeled into the crystal structures (see **Fig. S1**). All *S*-enantiomers occupy a space created by the aliphatic portions of lysine residues 29 and 32, with Leu28 and Val31 also in close proximity. The phenyl rings of *p*-tolyl and 3,5-dimethylphenyl occupy the exact same position. The 1-ethylpropyl, which has relatively poor inhibitory properties, had diffuse density (see **Fig. S1** for the density from omit maps), consistent with higher torsional freedom perhaps leading to the observed weaker inhibition. Its position closely agrees with that of the benzyl derivative. It is clear that any extensions beyond this

benzyl moiety would protrude from the binding site into solvent. This result defines the limit of what can be accommodated at the R_3 position of this inhibitor series.

These structures suggest that the complementarity of binding could be enhanced by modifying the aromatic portion of the dihydrophthalazine ring with a polar group or by including a hydrogen bond acceptor to interact with Arg57 (e.g., see the polar surface coloring used in **Fig. 2B**). Other derivatives incorporate methyl or methoxy groups at this distal position of the phthalazine (R_1 = R_2). Guided by the potency measurements, only the methoxy-modified inhibitors were included in crystallization trials. Co-crystallization with R_3 = *p*-methoxyphenyl (**12j**) revealed a poorer fit of the phthalazine into the crevice, with a 0.7 Å translation of this moiety upwards and out of the site (**Fig. 3A**, magenta). However, the R_3 group aligned perfectly with the *p*-tolyl (**11j**, light green) modification despite the change at the dihydrophthalazine edge. It seems likely, therefore, that simultaneous modifications at R_1 and R_2 are not ideal, as the lower portion of the phthalazine is already at the limits of what will fit in the binding site when only a hydrogen atom is present.

A previous structure determination of SaDHFR with a propyl-derivative of the current compound (R_3 = propyl, R_1 = R_2 = H; **11a**) series revealed conformational flexibility inherent in the acryloyl-based linker of the inhibitors, which allowed the dihydrophthalazine moiety to rotate into an alternate conformation [6]. The majority of the current structures do not contain convincing electron density to allow modeling into this shallow surface cavity. However, the exception is the R_1 = R_2 = OCH_3 derivatives of the dihydrophthalazine combined with an R_3 = cyclopropyl (**12c**), which surprisingly exhibits full occupancy of this alternative conformation. In this binding mode, the *R*-enantiomer of the R_3 modifications is favored, although the *S*-enantiomer still retains some electron density (approx. 60% is in the *R* state, with 40% in the *S* state, see **Table S2**). This non-canonical conformation is significantly less buried than the other inhibitors and is surrounded by hydrophobic residues Ile50, the aliphatic portion of Lys52, Leu54 underneath the dihydrophthalazine, and Pro55 (**Fig. 3B**, cyan). The methoxy groups at R_1 and R_2 do not appear to make any polar interactions, even with

ordered water molecules. Instead, they appear to provide a bulk that strains the fit within the canonical folate pocket. When the R_3 group is large, as with the *p*-methoxyphenyl modification (**12j**, **Fig. 3**, magenta), this strain in the canonical site is tolerated to allow a more favored placement of R_3. However, the smaller cyclopropyl moiety occupies a completely solvent-exposed position, seemingly to favor the binding of the dihydrophthalazine into the less-strained non-canonical site (**12c**, **Fig. 3B**, cyan). Over-filling of the folate pocket, therefore, is key to accessing the non-canonical shallow surface uniquely found in SaDHFR, and its complete occupancy has not been noted for any other inhibitors. Binding of inhibitors in this arrangement has a benefit of lessening the enantiomeric preference of the site, which would remove an eventual need downstream for the purification of racemic mixtures.

4. Conclusions

We have synthesized and evaluated methyl- and methoxy- dihydrophthalazine-appended DAP inhibitors for their ability to inhibit the DHFR enzyme and the whole cell growth of *S. aureus*. This series extends previous work with the *S. aureus* organism and reveals conservation of MIC values at or below 0.25 µg/mL, approximately 10-fold lower than the parent trimethoprim antibacterial [6]. The aryl groups appended to the dihydrophthalazine appear to hamper the permeability of the molecule, thus increasing the MIC values for these derivatives.

Important conclusions can be taken from the variations in inhibitors tested by defining a steric limit to modifications of the scaffold. For example, extensions beyond a benzyl moiety at R_3 result in poorer efficacy and likely distort the enzyme, precluding packing into a crystal form as observed for the co-crystallization attempt with R_3 = *p*-methoxybenzyl (R_1 = R_2 = H, **11p**). This allowed comparison of the site of hydration under the same crystallization conditions as that co-crystallized with inhibitors. The DAP ring is well suited to substitute for the observed conserved water network, likely driving the favorable interaction with all such DAP-containing inhibitors. Estimates of hydration effects in inhibitor binding can be up to 4.4 kcal/mol per contact [33]. In the current series, the strength and specificity of these interactions is likely highly important,

anchoring the scaffold in the site while alternative interactions are possible with the dihydrophthalazine moiety.

Structure determinations of co-crystallized SaDHFR with saturated racemic inhibitor solutions consistently yield weak density at the distal end of the dihydrophthalazine scaffold (**Fig. S1**). Interestingly, this seems to also be the case for the native folate substrate. Recent studies on time-resolved catalysis by the well-characterized DHFR from *E. coli* found similarly weak or diffuse electron density at this region of the pocket [34]. This, again, reinforces the importance of the polar interactions with water molecules, pterin heterocycles, or DAP ring structures to the binding energy and overall ordering within the pocket.

The previous observation of an alternate binding surface, found specifically in SaDHFR, has been confirmed in the current work [6]. The appending of additional bulk at the distal edge of the dihydrophthalazine creates a strained fit within the folate pocket, as seen in structure **12j** (R_1 = R_2 = OCH_3; R_3 = *p*-methoxyphenyl). However, this strain is apparently tolerated to gain favorable placement of the relatively hydrophobic R_3 moiety. When *p*-methoxyphenyl at R_3 is changed to a smaller cyclopropyl moiety (**12c**), the energetics balance with the strain imparted by the R_1 and R_2 methoxy groups. In this situation, the inhibitor is found to completely occupy the alternate binding site by rotating at the linker and placing the dihydrophthalazine on a hydrophobic ledge within the binding site. Furthermore, in this binding mode there is no observed preference for enantiomers at the chiral R_3 position. This novel insight then outlines the inhibitor design needed to maintain inhibitor potency while targeting this unique feature of the SaDHFR folate pocket.

5. Experimental

5.1 General methods

Commercial reagents were used directly as received. All reactions were performed under nitrogen in oven-dried glassware. All Grignard reagents were purchased from Sigma Aldrich. Commercial anhydrous (DMF) and dimethyl sulfoxide (DMSO) were stored under dry nitrogen and transferred by syringe when needed. Tetrahydrofuran

(THF) was dried over potassium hydroxide pellets and distilled from lithium aluminum hydride prior to use. Reactions were monitored by thin layer chromatography (TLC) on silica gel GF plates (Analtech, No. 21521) and visualized using a hand-held UV lamp. Preparative column chromatography was carried out on silica gel (Sorbent Technologies, 63-200 mesh) mixed with 0.5-1% UV-active phosphor (Sorbent Technologies, No. UV-05). Melting points were determined using a MEL-TEMP apparatus and were uncorrected. FT-IR spectra were run as dichloromethane solutions on NaCl disks. ^{1}H and ^{13}C NMR spectra were measured at 400 MHz and 100 MHz or 300 MHz and 75 MHz, respectively, in the indicated solvent unless specified. Chemical shifts (δ) are referenced to internal $(CH_3)_4Si$ and coupling constants (*J*) are given in Hz. Elemental analyses (± 0.4%) were performed by Atlantic Microlabs, Inc., Norcross, GA 30071.

*5.1.1. 3-Morpholinopropionitrile (**1**):* This compound was prepared on a 0.47 mol scale according to the literature procedure [27, 35]. The product was distilled at 88-90 ^{o}C/0.5 mm Hg (lit [35, 36] bp 149 ^{o}C/20 mm Hg) to give **1** (38.2 g, 95%) as a colorless liquid. IR: 2253 cm^{-1}; ^{1}H NMR ($CDCl_3$, 400 MHz): δ 3.72 (t, 4H, *J* = 4.7 Hz), 2.68 (t, 2H, *J* = 6.8 Hz), 2.52 (t, 2H, *J* = 7.0 Hz), 2.50 (t, 4H, *J* = 4.7 Hz); ^{13}C NMR (75 MHz): δ 118.6, 66.7, 53.6, 53.0, 15.7.

*5.1.2. 5-Iodo-3,4-dimethoxybenzaldehyde (**2**):* This compound was prepared on a 0.27-mol scale using the method of Nimgirawath [37]. The crude product was recrystallized (4:1 ethanol:water) to give **2** (25.2 g, 96%) as a white solid, mp 71-72 ^{o}C (lit [37] mp 71-72 ^{o}C). IR: 2832, 2730, 2693 cm^{-1}; ^{1}H NMR ($CDCl_3$, 300 MHz): δ 9.83 (s, 1H), 7.85 (d, 1H, *J* = 1.7 Hz), 7.41 (d, 1H, *J* = 1.7 Hz), 3.93 (s, 3H), 3.92 (s, 3H); ^{13}C NMR (75 MHz): δ 189.7, 154.2, 153.0, 134.7, 133.9, 111.0, 92.1, 60.7, 56.1.

*5.1.3. 2,4-Diamino-5-(5-iodo-3,4-dimethoxybenzyl)pyrimidine (**3**):* The general method of Roth *et al*. [38] was modified. To a stirred solution of **1** (6.92 g, 54.1 mmol) in DMSO (20 mL), NaOMe (0.29 g, 5.40 mmol) was added and heated at 70-72 ^{o}C. A pre-heated solution of **2** (12.2 g, 41.8 mmol) in DMSO (15 mL) was added to the reaction mixture dropwise over a period of 15 min and the reaction was heated for an additional 45 min. The crude reaction mixture was poured into cold ice water (50 mL) and extracted with DCM (3 × 100 mL). The combined organic layers were washed with satd. NaCl (100 mL), dried ($MgSO_4$) and concentrated under vacuum to give 3-morpholino-2-(5-iodo-3,4-dimethoxybenzyl)acrylonitrile (90%) as a dark red oil. The

crude material was further dissolved in ethanol (75 mL), followed by addition of aniline hydrochloride (6.76 g, 52.2 mmol), and refluxed for 1 h. During the reflux, guanidine hydrochloride (9.55 g, 100 mmol) and sodium methoxide (9.00 g, 167 mmol) were added and the reflux was continued for an additional 3 h. The reaction mixture was then concentrated to 1/3rd volume and cooled to 0 ^{o}C for 30 min. Addition of ice-cold water (40 mL) and stirring resulted in an off-white product as a precipitate. The resulting crude product was filtered, washed and recrystallized (EtOH:H_2O (4:1)) to give **3** (9.68 g, 60%) as a tan solid, mp 217-218 ^{o}C. IR: 3467, 3315, 3140, 1638 cm^{-1}; ^{1}H NMR (DMSO-d_6, 300 MHz): δ 7.57 (s, 1H), 7.14 (d, 1H, *J* = 1.8 Hz), 6.98 (d, 1H, *J* = 1.8 Hz), 6.16 (br s, 2H), 5.77 (br s, 2H), 3.77 (s, 3H), 3.66 (s, 3H), 3.54 (s, 2H); ^{13}C NMR (DMSO-d_6, 75 MHz): δ 162.4, 162.1, 156.0, 152.0, 146.3, 138.9, 129.1, 113.8, 105.2, 92.4, 59.8, 55.8, 31.7.

5.2.

*5.2.1. (±)-1-(6,7-Dimethoxy-1-ethylphthalazin-2(1H)-yl)prop-2-en-1-one (**9a**):* To a stirred solution of 6,7-dimethoxyphthalazine (**4**, 2.00 g, 16.3 mmol) [39] in dry THF (60 mL) at 0 ^{o}C, ethylmagnesium bromide (**6a**,12.6 mL, 12.6 mmol) was added dropwise over a period of 30 min. Stirring was continued at 0 ^{o}C for 30 min and continued at room temperature for 1 h. The reaction mixture was quenched with NH_4Cl (50 mL) and extracted with EtOAc (3 × 100 mL). The organic layer was washed with satd. NaCl (30 mL), dried ($MgSO_4$) and concentrated under vacuum to give the crude (±)-1,2-dihydro-1-ethyl-6,7-dimethoxyphthalazine (**7a**) as a viscous oil (90%). The material was taken to the next step without further purification.

To a stirred cooled solution of **7a** in DCM (150 mL), TEA (15.8 mL, 2.21 mmol) was added, followed by acryloyl chloride (0.95 mL, 11.6 mmol), and the reaction was stirred for 2 h. The reaction mixture was quenched with water (50 mL) and extracted with DCM (3 × 30 mL). The combined extracts were washed with satd. NaCl (50 mL), dried ($MgSO_4$) and concentrated under vacuum. The residue was purified on a column chromatography using silica gel with EtOAc:hexanes (3:7) to give **9a** (2.05 g, 57%) as a viscous, yellow oil. IR: 2839, 1659, 1614 cm^{-1}; ^{1}H NMR ($CDCl_3$, 300 MHz): δ 7.52 (s, 1H), 7.31 (dd, *J* = 17.2, 10.2 Hz, 1H), 6.79 (s, 1H), 6.67 (s, 1H), 6.46 (dd, *J* = 17.2, 1.9 Hz, 1H), 5.77 (dd, *J* = 10.2, 1.9 Hz, 1H), 5.74 (t, *J* = 6.6 Hz, 1H), 3.93 (s, 3H), 3.91 (s, 3H), 1.69 (m, 2H), 0.83 (t, *J* = 7.4 Hz, 3H); ^{13}C NMR ($CDCl_3$, 75 MHz): δ 166.2, 151.8, 148.6, 144.2, 128.1, 127.4, 127.3, 116.9, 109.2, 108.3, 56.12, 56.07, 52.1, 28.3, 9.6.

*5.2.2. (±)-1-(6,7-Dimethoxy-1-propylphthalazin-2(1H)-yl)prop-2-en-1-one (**9b**):* This compound was prepared using the same procedure as for **9a** above. Yield: 2.03 g (67%) as an off-white solid, mp 58-60 ^{o}C; IR: 2843, 1659, 1614 cm^{-1}; ^{1}H NMR ($CDCl_3$, 300 MHz): δ 7.53 (s, 1H), 7.29 (dd, *J* = 17.2, 10.2 Hz, 1H), 6.78 (s, 1H), 6.67 (s, 1H), 6.46 (d, *J* = 17.2 Hz, 1H), 5.78 (overlapping d, *J* = 10.1 Hz, 1H and t, *J* = 6.5 Hz, 1H),

3.93 (s, 3H), 3.91 (s, 3H), 1.61 (m, 2H), 1.27 (sextet, *J* = 7.3 Hz, 2H), 0.84 (t, *J* = 7.3 Hz, 3H); ^{13}C NMR ($CDCl_3$, 75 MHz): δ 166.3, 151.9, 148.6, 142.5, 128.2, 128.0, 127.3, 116.9, 109.2, 108.4, 56.2, 56.1, 50.9, 37.5, 18.5, 13.9.

*5.2.3. (±)-1-(1-Cyclopropyl-6,7-dimethoxyphthalazin-2(1H)-yl)prop-2-en-1-one (**9c**):* This compound was prepared using the same procedure as above. Yield: 2.48 g (66%) as a colorless viscous, yellow oil; IR: 2843, 1658, 1613 cm^{-1}; ^{1}H NMR ($CDCl_3$, 300 MHz): δ 7.58 (s, 1H), 7.35 (dd, *J* = 17.1, 10.5 Hz, 1H), 6.81 (s, 1H), 6.67 (s, 1H), 6.47 (dd, *J* = 17.1, 2.0 Hz, 1H), 5.79 (dd, *J* = 10.5, 2.0 Hz, 1H), 5.46 (d, *J* = 7.8 Hz, 1H), 3.94 (s, 3H), 3.92 (s, 3H), 1.17 (m, 1H), 0.58 (m, 1H), 0.43 (m, 2H), 0.32 (m, 1H); ^{13}C NMR ($CDCl_3$, 75 MHz): δ 166.4, 151.8, 148.7, 143.4, 128.0, 127.3, 126.5, 117.0, 109.2, 108.1, 56.1, 56.0, 53.5, 16.6, 3.5, 2.3.

*5.2.4. (±)-1-(6,7-Dimethoxy-1-vinylphthalazin-2(1H)-yl)prop-2-en-1-one (**9d**):* This compound was prepared using the same procedure as above. Yield: 2.07 g (58%) as a colorless oil; IR: 2852, 1661, 1614 cm^{-1}; ^{1}H NMR ($CDCl_3$, 300 MHz): δ 7.51 (s, 1H), 7.31 (dd, *J* = 17.3, 10.4 Hz, 1H), 6.79 (s, 1H), 6.71 (s, 1H), 6.49 (dd, *J* = 17.3, 1.6 Hz, 1H), 6.31 (d, *J* = 5.1 Hz, 1H), 5.82 (m, 1H), 5.79 (d, *J* = 10.2 Hz, 1H), 5.11 (d, *J* = 10.2 Hz, 1H), 4.89 (d, *J* = 17.0 Hz, 1H), 3.93 (s, 3H), 3.92 (s, 3H); ^{13}C NMR ($CDCl_3$, 75 MHz): δ 166.3, 152.1, 149.0, 141.7, 134.7, 128.6, 127.1, 125.6, 117.0, 116.3, 109.4, 108.5, 56.23, 56.16, 52.7.

*5.2.5. (±)-1-(6,7-Dimethoxy-1-(2-methylprop-1-en-1-yl)phthalazin-2(1H)-yl)prop-2-en-1-one (**9e**):* This compound was prepared using the same procedure as above. Yield: 1.95 g (62%) as an off-white solid, mp 52-54 °C; IR: 2836, 1660, 1609 cm^{-1}; ^{1}H NMR ($CDCl_3$, 300 MHz): δ 7.52 (s, 1H), 7.39 (dd, *J* = 17.0, 10.4 Hz, 1H), 6.77 (s, 1H), 6.60 (s, 1H), 6.45 (dd, *J* = 17.0, 1.5 Hz, 1H), 6.44 (d, *J* = 9.7 Hz, 1H), 5.75 (dd, *J* = 10.4, 1.5 Hz, 1H), 5.24 (d, *J* = 9.7 Hz, 1H), 3.92 (s, 3H), 3.90 (s, 3H), 2.02 (s, 3H), 1.65 (s, 3H); ^{13}C NMR ($CDCl_3$, 75 MHz): δ 166.0, 152.2, 148.7, 141.7, 134.1, 128.2, 128.0, 127.4, 122.3, 116.3, 108.6, 108.4, 56.1 (2C), 49.5, 25.7, 18.6.

*5.2.6. (±)-1-(6,7-Dimethoxy-1-phenylphthalazin-2(1H)-yl)prop-2-en-1-one (**9f**):* This compound was prepared using the same procedure as above. Yield: 1.85 g (56%) as a viscous, colorless oil; IR: 2835, 1660, 1609 cm^{-1}; ^{1}H NMR ($CDCl_3$, 300 MHz): δ 7.58 (s, 1H), 7.31 (dd, *J* = 17.2, 10.5 Hz, 1H), 7.26-7.17 (complex, 5H), 6.92 (s, 1H), 6.83 (s, 1H), 6.70 (s, 1H), 6.46 (dd, *J* = 17.5, 2.0 Hz, 1H), 5.76 (dd, *J* = 10.5, 2.1 Hz, 1H), 3.92 (s, 3H), 3.87 (s, 3H); ^{13}C NMR ($CDCl_3$, 75 MHz): δ 166.5, 152.3, 149.0, 141.8, 141.1, 128.6, 127.8, 127.3, 126.5, 116.8, 109.7, 108.4, 56.20, 56.16, 53.8 (two aromatic C unresolved).

*5.2.7. (±)-1-(6,7-Dimethoxy-1-(2-methylphenyl)phthalazin-2(1H)-yl)prop-2-en-1-one (**9g**)*: This compound was prepared using the same procedure as above. Yield: 2.04 g (58%) as a white solid, mp 73-75 °C; IR: 2835, 1662, 1616 cm^{-1}; ^{1}H NMR ($CDCl_3$, 300 MHz): δ 7.51 (s, 1H), 7.32 (dd, *J* = 17.2, 10.6 Hz, 1H), 7.18 (dd, *J* = 7.4, 1.6 Hz, 1H), 7.15-7.01 (complex, 3H), 6.90 (s, 1H), 6.78 (s, 1H), 6.54 (s, 1H), 6.38 (dd, *J* = 17.2, 2.1 Hz, 1H), 5.71 (dd, *J* = 10.5, 2.2 Hz, 1H), 3.89 (s, 3H), 3.81 (s, 3H), 2.73 (s, 3H); ^{13}C NMR ($CDCl_3$, 75 MHz): δ 166.4, 152.3, 148.7, 142.3, 140.0, 132.7, 130.7, 128.3, 128.1, 127.7, 127.6, 127.5, 126.8, 115.4, 108.8, 108.7, 56.1, 56.0, 52.0, 20.1.

*5.2.8. (±)-1-(1-(2-Ethylphenyl)-6,7-dimethoxyphthalazin-2(1H)-yl)prop-2-en-1-one (**9h**):* This compound was prepared using the same procedure as above. Yield: 1.90 g (53%) as a white solid, mp 69-71 °C; IR: 2830, 1663, 1616 cm^{-1}; ^{1}H NMR ($CDCl_3$, 300 MHz): δ 7.52 (s, 1H), 7.32 (dd, *J* = 17.2, 10.5 Hz, 1H), 7.19 (td, 2H, *J* = 7.8, 1.1 Hz), 7.15 (td, 1H, *J* = 7.8, 1.1 Hz), 7.03 (td, *J* = 7.4, 1.6 Hz, 1H), 6.97 (s, 1H), 6.78 (s, 1H), 6.58 (s, 1H), 6.38 (dd, *J* = 17.2, 2.1 Hz, 1H), 5.70 (dd, *J* = 10.5, 2.1 Hz, 1H), 3.89 (s, 3H), 3.80 (s, 3H), 3.18 (m, 2H), 1.41 (t, *J* = 7.4 Hz, 3H); ^{13}C NMR ($CDCl_3$, 75 MHz): δ 166.4, 152.3, 148.6, 141.4, 139.9, 128.6, 128.1, 127.84, 127.78, 127.6, 126.5, 115.5, 113.5, 109.1, 108.7, 56.1, 55.9, 51.5, 25.2, 15.6 (one aromatic C was unresolved).

*5.2.9. (±)-1-(6,7-Dimethoxy-1-(2-methoxyphenyl)phthalazin-2(1H)-yl)prop-2-en-1-one (**9i**):* This compound was prepared using the same procedure as above. Yield: 2.03 g (55%) as a white solid, mp 71-72 °C; IR: 2836, 1664, 1616 cm^{-1}; ^{1}H NMR ($CDCl_3$, 300 MHz): δ 7.51 (s, 1H), 7.39 (dd, *J* = 17.2, 10.5 Hz, 1H), 7.21-7.13 (complex, 3H), 7.04 (s, 1H), 6.86 (d, *J* = 8.2 Hz, 1H), 6.81 (t, *J* = 7.4 Hz, 1H), 6.72 (s, 1H), 6.40 (dd, *J* = 17.2, 2.0 Hz, 1H), 5.76 (dd, *J* = 10.5, 2.2 Hz, 1H), 3.96 (s, 3H), 3.86 (s, 6H); ^{13}C NMR ($CDCl_3$, 75 MHz): δ 166.3, 154.9, 152.0, 148.6, 140.6, 132.1, 128.9, 128.4, 128.0, 127.4, 126.6, 121.3, 115.6, 111.3, 109.4, 108.5, 56.1, 55.9, 55.8, 49.9.

*5.2.10. (±)-1-(6,7-Dimethoxy-1-(4-methoxyphenyl)phthalazin-2(1H)-yl)prop-2-en-1-one (**9j**):* This compound was prepared using the same procedure as above. Yield: 2.10 g (59%) as a yellow solid, mp 55-56 °C; IR: 2836, 1659, 1609 cm^{-1}; ^{1}H NMR ($CDCl_3$, 300 MHz): δ 7.58 (s, 1H), 7.28 (dd, *J* = 17.2, 10.5 Hz, 1H), 7.14 (d, *J* = 9.0 Hz, 2H), 6.89 (s, 1H), 6.84 (s, 1H), 6.77 (d, *J* = 9.0 Hz, 2H), 6.67 (s, 1H), 6.45 (dd, *J* = 17.2, 2.2 Hz, 1H), 5.75 (dd, *J* = 10.5, 2.2 Hz, 1H), 3.93 (s, 3H), 3.87 (s, 3H), 3.73 (s, 3H); ^{13}C NMR ($CDCl_3$, 75 MHz): δ 166.5, 159.1, 152.4, 149.0, 141.8, 133.6, 128.8, 128.5, 127.4, 126.8, 116.9, 113.9, 109.6, 108.3, 56.21, 56.20, 55.3, 53.2.

5.3.

*5.3.1. (±)-1-(1-Ethyl-6,7-dimethylphthalazin-2(1H)-yl)prop-2-en-1-one (**10a**)*: This compound was prepared with dimethylphthalazine (**5**) [39] using the same procedure as

for **9a** above. Yield: 2.29 g (60%) as a viscous, colorless oil; IR: 1663, 1619 cm^{-1}; ^{1}H NMR ($CDCl_3$, 300 MHz): δ 7.52 (s, 1H), 7.32 (dd, *J* = 17.2, 10.5 Hz, 1H), 7.02 (s, 1H), 6.91 (s, 1H), 6.45 (dd, *J* = 17.2, 2.3 Hz, 1H), 5.75 (dd, *J* = 10.5, 2.3 Hz, 1H), 5.74 (t, *J* = 7.1 Hz, 1H), 2.29 (s, 3H), 2.26 (s, 3H), 1.63 (m, 2H), 0.81 (t, *J* = 7.5 Hz, 3H); ^{13}C NMR ($CDCl_3$, 75 MHz): δ 166.3, 142.6, 140.7, 136.4, 131.4, 128.0, 127.7, 127.4, 126.8, 121.9, 52.3, 28.4, 20.1, 19.5, 9.5.

*5.3.2. (±)-1-(6,7-Dimethyl-1-propylphthalazin-2(1H)-yl)prop-2-en-1-one (**10b**):* This compound was prepared using the same procedure as above. Yield: 2.26 g (70%) as an off-white solid, mp 62-64 ^{o}C; IR: 1663, 1619 cm^{-1}; ^{1}H NMR ($CDCl_3$, 300 MHz): δ 7.55 (s, 1H), 7.30 (dd, *J* = 17.2, 10.5 Hz, 1H), 7.04 (s, 1H), 6.92 (s, 1H), 6.43 (dd, *J* = 17.2, 2.3 Hz, 1H), 5.77 (t, *J* = 6.7 Hz, 1H), 5.75 (dd, *J* = 10.5, 2.3 Hz, 1H), 2.29 (s, 3H), 2.27 (s, 3H), 1.59 (m, 2H), 1.25 (sextet, *J* = 7.3 Hz, 2H), 0.85 (t, *J* = 7.4 Hz, 3H); ^{13}C NMR ($CDCl_3$, 75 MHz): δ 166.2, 142.8, 140.8, 136.4, 131.9, 128.1, 127.6, 127.4, 126.8, 121.8, 51.0, 37.6, 20.1, 19.5, 18.3, 13.9.

*5.3.3. (±)-1-(1-Cyclopropyl-6,7-dimethylphthalazin-2(1H)-yl)prop-2-en-1-one (**10c**):* This compound was prepared using the same procedure as above. Yield: 2.61 g (65%) as a yellow oil; IR: 1666, 1619 cm^{-1}; ^{1}H NMR ($CDCl_3$, 300 MHz): δ 7.60 (s, 1H), 7.33 (dd, *J* = 17.2, 10.5 Hz, 1H), 7.06 (s, 1H), 6.92 (s, 1H), 6.45 (dd, *J* = 17.2, 2.0 Hz, 1H), 5.77 (dd, *J* = 10.5, 2.0 Hz, 1H), 5.42 (d, *J* = 8.2 Hz, 1H), 2.31 (s, 3H), 2.28 (s, 3H), 1.16 (m, 1H), 0.60 (m, 1H), 0.41 (m, 2H), 0.30 (m, 1H); ^{13}C NMR ($CDCl_3$, 75 MHz): δ 166.6, 142.9, 141.0, 136.7, 130.7, 128.2, 127.7, 127.5, 126.7, 122.0, 53.8, 20.2, 19.6, 16.8, 3.8, 2.4.

*5.3.4. (±)-1-(6,7-Dimethyl-1-vinylphthalazin-2(1H)-yl)prop-2-en-1-one (**10d**):* This compound was prepared using the same procedure as above. Yield**:** 1.85 g (61%) as a viscous, yellow oil; IR: 1664, 1619 cm^{-1}; ^{1}H NMR ($CDCl_3$, 300 MHz): δ 7.52 (s, 1H), 7.32 (dd, *J* = 17.2, 10.5 Hz, 1H), 7.06 (s, 1H), 6.98 (s, 1H), 6.51 (dd, *J* = 17.2, 1.9 Hz, 1H), 6.30 (d, *J* = 4.7 Hz, 1H), 5.80 (m, 1H), 5.79 (dd, *J* = 10.5, 1.9 Hz, 1H), 5.08 (d, *J* = 9.2 Hz, 1H), 4.88 (d, *J* = 16.8 Hz, 1H), 2.30 (s, 3H), 2.28 (s, 3H); ^{13}C NMR ($CDCl_3$, 75 MHz): δ 166.3, 142.1, 141.2, 137.0, 135.1, 129.7, 128.7, 128.0, 127.2, 127.0, 121.7, 115.9, 53.0, 20.2, 19.6.

*5.3.5. (±)-1-(6,7-Dimethyl-1-(2-methylprop-1-en-1-yl)phthalazin-2(1H)-yl)prop-2-en-1-one (**10e**):* This compound was prepared using the same procedure as above. Yield: 2.71 g (66%) as an off-white solid, mp 51-53 °C; IR: 1666, 1619 cm^{-1}; ^{1}H NMR ($CDCl_3$, 300 MHz): δ 7.52 (s, 1H), 7.29 (dd, *J* = 17.2, 10.5 Hz, 1H), 7.02 (s, 1H), 6.88 (s, 1H), 6.45 (dd, *J* = 17.3, 2.0 Hz, 1H), 6.43 (d, *J* = 10.0 Hz, 1H), 5.99 (dd, *J* = 10.5, 2.0 Hz, 1H), 5.24 (d, *J* = 10.0 Hz, 1H), 2.27 (s, 3H), 2.25 (s, 3H), 2.02 (s, 3H), 1.63 (s, 3H); ^{13}C

NMR ($CDCl_3$, 75 MHz): δ 166.0, 141.9, 141.3, 136.4, 133.9, 132.2, 128.0, 127.5, 127.2, 126.9, 122.4, 121.0, 49.7, 25.7, 20.1, 19.5, 18.6.

*5.3.6. (±)-1-(6,7-Dimethyl-1-phenylphthalazin-2(1H)-yl)prop-2-en-1-one (**10f**):* This compound was prepared using the same procedure as above: Yield: 2.10 g (58%) as a white solid, mp 69-70 ^{o}C; IR: 1663, 1618 cm^{-1}; ^{1}H NMR ($CDCl_3$, 300 MHz): δ 7.59 (s, 1H), 7.32 (dd, *J* = 17.2, 10.5 Hz, 1H), 7.26-7.15 (complex, 5H), 7.10 (s, 1H), 7.00 (s, 1H), 6.88 (s, 1H), 6.45 (dd, *J* = 17.2, 1.9 Hz, 1H), 5.76 (dd, *J* = 10.5, 1.9 Hz, 1H), 2.27 (s, 3H), 2.26 (s, 3H); ^{13}C NMR ($CDCl_3$, 75 MHz): δ 166.4, 142.0, 141.54, 141.50, 136.9, 130.7, 128.6 (2C), 128.3, 127.7, 127.3, 127.0, 121.4, 54.2, 20.2, 19.5 (one aromatic C unresolved).

5.4.

*5.4.1. Synthesis of Derivatives **11a-q**.* The preparation of these compounds was previously reported [27].

*5.4.2. (±)-(E)-3-(5-((2,4-Diaminopyrimidin-5-yl)methyl)-2,3-dimethoxyphenyl)-1-(1-ethyl-6,7-dimethoxyphthalazin-2(1H)-yl)prop-2-en-1-one (**12a**):* To stirred solution of 2,4-diamino-5-(5-iodo-3,4-dimethoxybenzyl)pyrimidine (**3**) (2.50 g, 6.47 mmol) in dry DMF (25 mL), (±)-1-(6,7-dimethoxy-1-ethylphthalazin-2(*1H*)-yl)prop-2-en-1-one (**9a**) (2.23 g, 7.76 mmol), palladium acetate (0.143 g, 0.64 mmol), and *N*-ethylpiperidine (2.67 mL, 19.4 mmol) were added at heated at 120 ^{o}C for 12 h. After completion, the reaction mixture was poured into ice-cold water (40 mL) and extracted EtOAc (4 × 20 mL). The organic layers were combined, washed with satd. NaCl (50 mL), dried ($MgSO_4$) and concentrated under vacuum to give the crude product. The dark brown residue was purified by silica gel chromatography eluted with MeOH:DCM:TEA by silica gel chromatography (5:94:1) to furnish a yellow solid. This solid was further purified by recrystallization from MeOH:Et_2O (2:3) to give **12a** (2.02 g, 59%) as a white solid, mp 215-217 °C. IR: 3424, 3334, 3145, 3105, 2839, 1657, 1638, 1600 cm^{-1}; ^{1}H NMR (DMSO-d_6, 300 MHz): δ 7.85 (d, *J* = 16.0 Hz, 1H), 7.78 (s, 1H), 7.63 (d, *J* = 16.0 Hz, 1H), 7.59 (s, 1H), 7.24 (d, *J* = 1.5 Hz, 1H), 7.11 (s, 1H), 7.05 (s, 1H), 6.98 (d, *J* = 1.5 Hz, 1H), 6.27 (br s, 2H), 5.81 (br s, 2H), 5.75 (t, *J* = 6.3 Hz, 1H), 3.83 (s, 3H), 3.80 (s, 3H), 3.79 (s, 3H), 3.73 (s, 3H), 3.59 (s, 2H), 1.60 (m, 2H), 0.74 (t, *J* = 7.4 Hz, 3H); ^{13}C NMR (DMSO-d_6, 75 MHz): δ 165.5, 162.2, 161.8, 154.9, 152.4, 152.6, 148.2, 145.9, 142.5, 136.4, 136.1, 127.8, 126.8, 118.2, 118.0, 116.5, 114.6, 109.8, 109.0, 105.8, 60.7, 55.7, 55.6, 55.5, 51.3, 32.3, 27.8, 9.3. Anal. Calcd for $C_{28}H_{32}N_6O_5 \cdot 1.0\ H_2O$: C, 61.08; H, 6.22; N, 15.26. Found: C, 61.16; H, 6.01; N, 15.11.

*5.4.3. (±)-(E)-3-(5-((2,4-Diaminopyrimidin-5-yl)methyl)-2,3-dimethoxyphenyl)-1-(6,7-dimethoxy-1-propylphthalazin-2(1H)-yl)prop-2-en-1-one (**12b**):* This compound was

prepared using the same procedure as for **12a** above. Yield: 2.18 g (62%) as a white solid, mp 228-230 °C; IR: 3356, 3222, 3160, 2838, 1662, 1633, 1606 cm^{-1}; ^{1}H NMR (DMSO-d_6, 400 MHz): δ 7.86 (d, *J* = 16.1 Hz, 1H), 7.82 (s, 1H), 7.64 (d, *J* = 16.1 Hz, 1H), 7.58 (s, 1H), 7.38 (s, 1H), 7.14 (s, 1H), 7.05 (s, 1H), 7.01 (s, 1H), 6.88 (br s, 2H), 6.40 (br s, 2H), 5.81 (t, *J* = 6.4 Hz, 1H), 3.84 (s, 3H), 3.80 (s, 6H), 3.75 (s, 3H), 3.63 (s, 2H), 1.53 (m, 2H), 1.19 (sextet, *J* = 7.5 Hz, 2H), 0.82 (t, *J* = 7.4 Hz, 3H); ^{13}C NMR (DMSO-d_6, 101 MHz): δ 164.9, 162.3, 152.0, 151.1, 147.7, 145.5, 142.3, 135.6, 134.9, 127.4, 126.8, 118.0, 117.6, 115.9, 114.2, 109.2, 108.6, 106.4, 60.2, 55.3, 55.2, 55.1, 49.5, 36.5, 31.5, 17.3, 13.2 (two aromatic C unresolved). Anal. Calcd for $C_{29}H_{34}N_6O_5 \cdot 4.5\ H_2O$: C, 55.49; H, 6.31; N, 13.39. Found: C, 55.89; H, 6.00; N, 13.75.

*5.4.4. (±)-(E)-1-(1-Cyclopropyl-6,7-dimethoxyphthalazin-2(1H)-yl)-3-(5-((2,4-diaminopyrimidin-5-yl)methyl)-2,3-dimethoxyphenyl)prop-2-en-1-one (**12c**):* This compound was prepared using the same procedure as above. Yield: 1.05 g (50%) as a white solid, mp 125-127 °C; IR: 3363, 3213, 3170, 2836, 1650, 1635, 1605 cm^{-1}; ^{1}H NMR (DMSO-d_6, 300 MHz): δ 7.84 (s, 1H and d, *J* = 16.0 Hz, 1H), 7.65 (d, *J* = 16.0 Hz, 1H), 7.57 (s, 1H), 7.26 (s, 1H), 7.14 (s, 1H), 7.10 (s, 1H), 7.00 (s, 1H), 6.73 (br s, 2H), 6.25 (br s, 2H), 5.39 (d, *J* = 8.2 Hz, 1H), 3.83 (s, 3H), 3.80 (s, 3H), 3.79 (s, 3H), 3.74 (s, 3H), 3.61 (s, 2H), 1.08 (m, 1H), 0.48 (m, 2H), 0.40 (m, 1H), 0.31 (m, 1H); ^{13}C NMR (DMSO-d_6, 75 MHz): δ 165.8, 162.7, 159.9, 152.6, 151.8, 151.1, 148.4, 146.1, 143.0, 136.3, 135.7, 128.0, 126.5, 118.6, 118.3, 116.7, 114.8, 110.0, 109.0, 106.7, 60.8, 55.9, 55.8, 55.7, 53.0, 32.2, 16.6, 3.8, 2.0. Anal. Calcd for $C_{29}H_{32}N_6O_5 \cdot 2.9\ H_2O$: C, 58.36; H, 5.93; N, 14.08. Found: C, 58.15; H, 5.72; N, 13.69.

*5.4.5. (±)-(E)-3-(5-((2,4-Diaminopyrimidin-5-yl)methyl)-2,3-dimethoxyphenyl)-1-(6,7-dimethoxy-1-vinylphthalazin-2(1H)-yl)prop-2-en-1-one (**12d**):* This compound was prepared using the same procedure as above. Yield: 1.14 g (52%) as a white solid, mp 210-212 °C; IR: 3341, 3158, 3082, 2842, 1667, 1637, 1629 cm^{-1}; ^{1}H NMR (DMSO-d_6, 300 MHz): δ 7.85 (d, *J* = 16.2 Hz, 1H), 7.75 (s, 1H), 7.66 (d, *J* = 16.2 Hz, 1H), 7.62 (br s, 2H), 7.54 (s, 1H), 7.31 (s, 1H), 7.13 (br s, 4H), 7.02 (s, 1H), 6.29 (d, *J* = 3.5 Hz, 1H), 5.76 (m, 1H), 5.03 (dd, *J* = 10.1, 1.1 Hz, 1H), 4.77 (dd, *J* = 16.8, 1.1 Hz, 1H), 3.81 (s, 3H), 3.78 (2s, 6H), 3.73 (s, 3H), 3.63 (s, 2H); ^{13}C NMR (DMSO-d_6, 75 MHz): δ 165.5, 163.6, 156.1, 152.7, 151.9, 148.5, 146.3, 146.0, 142.2, 136.5, 135.4, 134.4, 128.0, 125.3, 118.9, 118.1, 116.4, 115.0, 114.9, 110.0, 109.3, 108.2, 60.8, 55.89, 55.85, 55.7, 52.1, 31.8. Anal. Calcd for $C_{28}H_{30}N_6O_5 \cdot 4.1\ H_2O$: C, 54.67; H, 5.92; N, 13.84. Found: C, 54.88; H, 5.72; N, 13.84.

*5.4.6. (±)-(E)-3-(5-((2,4-Diaminopyrimidin-5-yl)methyl)-2,3-dimethoxyphenyl)-1-(6,7-dimethoxy-1-(2-methylprop-1-en-1-yl)phthalazin-2(1H)-yl)prop-2-en-1-one (**12e**):* This compound was prepared using the same procedure as above. Yield: 1.45 g (56%) as a

yellow solid, mp 212-213 °C; IR: 3466, 3324, 3150, 3100, 2838, 1643, 1598 cm^{-1}; ^{1}H NMR (DMSO-d_6, 400 MHz): δ 7.80 (overlapping s, 1H and d, *J* = 15.4 Hz, 1H), 7.58 (overlapping s, 1H and d, *J* = 15.4 Hz, 1H), 7.22 (s, 1H), 7.13 (s, 1H), 6.98 (s, 1H), 6.87 (s, 1H), 6.43 (d, *J* = 9.7 Hz, 1H), 6.18 (br s, 2H), 5.74 (br s, 2H), 5.19 (d, *J* = 9.7 Hz, 1H), 3.82 (s, 3H), 3.80 (2s, 6H), 3.74 (s, 3H), 3.60 (s, 2H), 1.97 (s, 3H), 1.60 (s, 3H); ^{13}C NMR (DMSO d_6, 101 MHz): δ 164.6, 161.7, 161.6, 155.2, 151.9, 151.4, 147.8, 145.4, 141.7, 136.0, 135.8, 132.7, 127.3, 126.8, 121.8, 117.7, 117.5, 115.5, 114.1, 108.7, 108.4, 105.1, 60.2, 55.2, 55.1, 48.2, 31.8, 24.8, 17.9 (one OCH_3 unresolved). Anal. Calcd for $C_{30}H_{34}N_6O_5 \cdot 1.5\ H_2O$: C, 61.53; H, 6.37; N, 14.35. Found: C, 61.27; H, 6.32; N, 14.43.

*5.4.7. (±)-(E)-3-(5-((2,4-Diaminopyrimidin-5-yl)methyl)-2,3-dimethoxyphenyl)-1-(6,7-dimethoxy-1-phenylphthalazin-2(1H)-yl)prop-2-en-1-one (**12f**):* This compound was prepared using the same procedure as above. Yield: 1.74 g (58%) as a white solid, mp 190-192 °C; IR: 3455, 3385, 3339, 3183, 2839, 1654, 1612 cm^{-1}; ^{1}H NMR (DMSO-d_6, 300 MHz): δ 7.86 (s, 1H), 7.85 (d, *J* = 16.0 Hz, 1H), 7.68 (d, *J* = 16.0 Hz, 1H), 7.60 (s, 1H), 7.31-7.19 (complex, 7H), 7.17 (s, 1H), 6.98 (d, *J* = 16.0 Hz, 1H), 6.94 (s, 1H), 6.17 (br s, 2H), 5.72 (br s, 2H), 3.82 (s, 3H), 3.80 (s, 3H), 3.78 (s, 3H), 3.73 (s, 3H), 3.59 (s, 2H); ^{13}C NMR (DMSO-d_6, 75 MHz): δ 165.7, 162.3, 162.1, 155.8, 152.5, 152.1, 148.5, 146.0, 142.3, 141.6, 136.8, 136.6, 128.5, 127.7, 127.4, 126.3, 126.2, 118.3, 117.8, 116.1, 114.8, 110.2, 109.3, 105.7, 60.8, 55.9, 55.72, 55.67, 53.2, 32.4. Anal. Calcd for $C_{32}H_{32}N_6O_5 \cdot 0.7\ H_2O$: C, 64.79; H, 5.67; N, 14.17. Found: C, 64.75; H, 5.67; N, 14.08.

*5.4.8. (±)-(E)-3-(5-((2,4-Diaminopyrimidin-5-yl)methyl)-2,3-dimethoxyphenyl)-1-(6,7-dimethoxy-1-(2-methylphenyl)phthalazin-2(1H)-yl)prop-2-en-1-one (**12g**):* This compound was prepared using the same procedure as above. Yield: 2.10 (55%) as a yellow solid, mp 179-180 °C; IR: 3466, 3330, 3099, 2835, 1669, 1643, 1603 cm^{-1}; ^{1}H NMR (DMSO-d_6, 300 MHz): δ 7.84 (s, 1H), 7.79 (d, *J* = 16.0 Hz, 1H), 7.64 (d, *J* = 16.0 Hz, 1H), 7.60 (s, 1H), 7.25 (s, 1H), 7.19 (s, 1H), 7.18-7.03 (complex, 4H), 6.97 (s, 1H), 6.90 (s, 1H), 6.73 (s, 1H), 6.21 (br s, 2H), 5.77 (br s, 2H), 3.80 (s, 3H), 3.77 (s, 3H), 3.75 (s, 3H), 3.70 (s, 3H), 3.59 (s, 2H), 2.73 (s, 3H); ^{13}C NMR (DMSO-d_6, 75 MHz): δ 165.6, 162.21, 162.19, 155.5, 152.5, 152.0, 148.4, 146.0, 142.8, 140.7, 136.5, 133.9, 130.4, 127.8, 127.3, 126.9, 126.7, 118.2, 118.0, 115.2, 114.7, 109.7, 109.0, 105.8, 60.8, 55.72, 55.68, 51.1, 32.4, 19.7 (1 aromatic C and 1 OCH_3 were unresolved). Anal. Calcd for $C_{33}H_{34}N_6O_5 \cdot 1.7\ H_2O$: C, 63.39; H, 5.98; N, 13.44. Found: C, 63.52; H, 5.68; N, 13.69.

*5.4.9. (±)-(E)-3-(5-((2,4-Diaminopyrimidin-5-yl)methyl)-2,3-dimethoxyphenyl)-1-(1-(2-ethylphenyl)-6,7-dimethoxyphthalazin-2(1H)-yl)prop-2-en-1-one (**12h**):* This compound was prepared using the same procedure as above. Yield: 1.29 g (56%) as a white solid, mp 147-149 °C; IR: 3455, 3328, 3101, 2834, 1669, 1647, 1606 cm^{-1}; ^{1}H NMR (DMSO-

d_6, 400 MHz): δ 7.82 (s, 1H), 7.79 (d, *J* = 16.1 Hz, 1H), 7.65 (d, *J* = 16.1 Hz, 1H), 7.60 (s, 1H), 7.24 (s, 1H), 7.24-7.02 (complex, 4H), 7.18 (s, 1H), 6.98 (s, 1H), 6.97 (s, 1H), 6.73 (s, 1H), 6.17 (br s, 2H), 5.73 (br s, 2H), 3.80 (s, 3H), 3.77 (s, 3H), 3.73 (s, 3H), 3.70 (s, 3H), 3.59 (s, 2H), 3.16 (m, 2H), 1.36 (t, *J* = 7.5 Hz, 3H); ^{13}C NMR (DMSO-*d_6*, 75 MHz): δ 165.4, 162.2, 162.1, 155.7, 152.4, 151.8, 148.3, 145.9, 141.9, 140.7, 139.5, 136.5, 136.4, 128.3, 127.7, 127.5, 127.2, 126.9, 126.3, 118.1, 118.0, 115.1, 114.6, 109.6, 109.0, 105.6, 60.7, 55.62, 55.57, 55.5, 50.6, 32.3, 24.4, 15.3. Anal. Calcd for $C_{34}H_{36}N_6O_5 \cdot 3.0\ H_2O$: C, 58.70; H, 5.12; N, 14.08. Found: C, 58.49; H, 4.81; N, 14.51.

*5.4.10. (±)-(E)-3-(5-((2,4-Diaminopyrimidin-5-yl)methyl)-2,3-dimethoxyphenyl)-1-(6,7-dimethoxy-1-(2-methoxyphenyl)phthalazin-2(1H)-yl)prop-2-en-1-one (**12i**):* This compound was prepared using the same procedure as above. Yield: 1.55 g (58%) as a yellow solid, mp 257-259 °C; IR: 3486, 3376, 3177, 2833, 1659, 1606 cm^{-1}; ^{1}H NMR (DMSO-*d_6*, 300 MHz): δ 7.82 (s, 1H), 7.81 (d, *J* = 16.0 Hz, 1H), 7.74 (d, *J* = 16.0 Hz, 1H), 7.62 (s, 1H), 7.29 (s, 1H), 7.19 (t, *J* = 7.8 Hz, 1H), 7.15 (s, 1H), 7.10 (s, 1H), 7.09 (s, 1H), 7.08 (dd, *J* = 7.8, 1.2 Hz, 1H), 7.01 (d, *J* = 7.8 Hz, 1H), 6.99 (d, J = 1.5 Hz, 1H), 6.81 (t, *J* = 7.8 Hz, 1H), 6.20 (br s, 2H), 5.75 (br s, 2H), 3.95 (s, 3H), 3.81 (s, 3H), 3.78 (s, 3H), 3.77 (s, 3H), 3.71 (s, 3H), 3.61 (s, 2H); ^{13}C NMR (DMSO-*d_6*, 75 MHz): δ 165.6, 162.3, 162.2, 155.8, 154.5, 152.5, 151.7, 148.3, 146.0, 141.0, 136.7, 136.6, 131.8, 128.8, 127.7, 126.8, 125.5, 120.0, 118.2, 117.9, 115.3, 114.7, 111.4, 109.5, 109.1, 105.8, 60.8, 55.9, 55.72, 55.68, 55.0, 52.6, 32.4. Anal. Calcd for $C_{33}H_{34}N_6O_6 \cdot 1.0\ H_2O$: C, 63.05; H, 5.77; N, 13.37. Found: C, 63.02; H, 5.84; N, 13.21.

*5.4.11. (±)-(E)-3-(5-((2,4-Diaminopyrimidin-5-yl)methyl)-2,3-dimethoxyphenyl)-1-(6,7-dimethoxy-1-(4-methoxyphenyl)phthalazin-2(1H)-yl)prop-2-en-1-one (**12j**):* This compound was prepared using the same procedure as above. Yield: 1.70 g (60%) as a pale yellow solid, mp 223-224 °C; IR: 3476, 3393, 3317, 3184, 2839, 1657, 1609 cm^{-1}; ^{1}H NMR (DMSO-*d_6*, 300 MHz): δ 7.87 (d, *J* = 16.0 Hz, 1H), 7.87 (s, 1H), 7.67 (d, *J* = 16.0 Hz, 1H), 7.61 (s, 1H), 7.26 (s, 1H), 7.18 (s, 1H), 7.17 (s, 1H), 7.13 (d, *J* = 8.6 Hz, 2H), 6.99 (s, 1H), 6.90 (s, 1H), 6.83 (d, *J* = 8.6 Hz, 2H), 6.20 (br s, 2H), 5.76 (br s, 2H), 3.81 (2s, 6H), 3.79 (s, 3H), 3.73 (s, 3H), 3.68 (s, 3H), 3.60 (s, 2H); ^{13}C NMR (DMSO-*d_6*, 75 MHz): δ 165.7, 162.3, 162.2, 158.5, 155.8, 152.5, 152.1, 148.5, 146.0, 142.3, 136.7, 136.6, 133.8, 127.8, 127.7, 126.6, 118.3, 117.9, 116.2, 114.7, 113.8, 110.1, 109.2, 105.8, 60.8, 55.9, 55.73, 55.68, 55.0, 52.6, 32.4. Anal. Calcd for $C_{33}H_{34}N_6O_6 \cdot 0.4\ H_2O$: C, 64.15; H, 5.68; N, 13.60. Found: C, 64.38; H, 5.67; N, 13.61.

5.5.

*5.5.1. (±)-(E)-3-(5-((2,4-Diaminopyrimidin-5-yl)methyl)-2,3-dimethoxyphenyl)-1-(1-ethyl-6,7-dimethylphthalazin-2(1H)-yl)prop-2-en-1-one (**13a**):* This compound was prepared

using the same procedure as for **12a** above. Yield: 1.45 g (56%) as a white solid, mp 210-212 °C. IR: 3425, 3350, 3171, 1667, 1634, 1605 cm^{-1}; ^{1}H NMR (DMSO-d_6, 300 MHz): δ 7.84 (d, *J* = 16.0 Hz, 1H), 7.80 (s, 1H), 7.63 (d, *J* = 16.0 Hz, 1H), 7.57 (s, 1H), 7.25 (s, 2H), 7.15 (s, 1H), 7.00 (s, 1H), 6.58 (br s, 2H), 6.11 (br s, 2H), 5.68 (t, *J* = 6.3 Hz, 1H), 3.79 (s, 3H), 3.73 (s, 3H), 3.60 (s, 2H), 2.27 (s, 3H), 2.25 (s, 3H), 1.57 (m, 2H), 0.72 (t, *J* = 7.5 Hz, 3H); ^{13}C NMR (DMSO-d_6, 75 MHz): δ 164.9, 162.0, 159.9, 151.9, 145.4, 142.0, 140.0, 135.7 (2C), 135.6, 135.3, 130.2, 127.3, 126.9, 126.2, 121.0, 117.9, 117.5, 114.2, 105.8, 60.2, 55.2, 50.9, 31.6, 27.4, 19.1, 18.5, 8.7. Anal. Calcd for $C_{28}H_{32}N_6O_3 \cdot 2.0\ H_2O$: C, 62.67; H, 6.76; N, 15.66. Found: C, 62.66; H, 6.36; N, 15.53.

*5.5.2. (±)-(E)-3-(5-((2,4-Diaminopyrimidin-5-yl)methyl)-2,3-dimethoxyphenyl)-1-(6,7-dimethyl-1-propylphthalazin-2(1H)-yl)prop-2-en-1-one (**13b**):* The compound was prepared using the same procedure as above. Yield: 1.52 g (52%) as a white solid, mp 228-230 °C; IR: 3354, 3164, 1667, 1638, 1607 cm^{-1}; ^{1}H NMR (DMSO-d_6, 300 MHz): δ 7.82 (s, 1H), 7.77 (d, *J* = 16.0 Hz, 1H), 7.62 (d, *J* = 16.0 Hz, 1H), 7.57 (s, 1H), 7.25 (s, 1H), 7.23 (d, *J* = 1.6 Hz, 1H), 7.14 (s, 1H), 6.99 (d, *J* = 1.5 Hz, 1H), 6.39 (br s, 2H), 5.93 (br s, 2H), 5.74 (t, *J* = 6.5 Hz, 1H), 3.78 (s, 3H), 3.73 (s, 3H), 3.59 (s, 2H), 2.27 (s, 3H), 2.24 (s, 3H), 1.48 (m, 2H), 1.16 (sextet, *J* = 7.5 Hz, 2H), 0.80 (t, *J* = 7.4 Hz, 3H); ^{13}C NMR (DMSO-d_6, 75 MHz): δ 164.9, 161.9, 160.4, 152.8, 151.9, 145.4, 142.2, 140.1, 135.8, 135.7, 135.5, 130.7, 127.3, 126.8, 126.2, 120.9, 117.8, 117.5, 114.1, 105.6, 60.2, 55.2, 49.6, 36.5, 31.7, 19.1, 18.5, 17.2, 13.1. Anal. Calcd for $C_{29}H_{34}N_6O_3 \cdot 1.7\ H_2O$: C, 63.88; H, 6.91; N, 15.41 Found: C, 63.72; H, 6.59; N, 15.02.

*5.5.3. (±)-(E)-1-(1-Cyclopropyl-6,7-dimethylphthalazin-2(1H)-yl)-3-(5-((2,4-diaminopyrimidin-5-yl)methyl)-2,3-dimethoxyphenyl)prop-2-en-1-one (**13c**):* This compound was prepared using the same procedure as above. Yield: 1.48 g (51%) as a white solid, mp 125-127 °C; IR: 3357, 3165, 1660, 1646, 1608, 1596 cm^{-1}; ^{1}H NMR (DMSO-d_6, 300 MHz): δ 7.87 (s, 1H), 7.84 (d, *J* = 16.0 Hz, 1H), 7.65 (d, *J* = 16.0 Hz, 1H), 7.58 (s, 1H), 7.25 (m, 2H), 7.19 (s, 1H), 7.00 (d, *J* = 1.4 Hz, 1H), 6.69 (br s, 2H), 6.22 (br s, 2H), 5.34 (d, *J* = 8.2 Hz, 1H), 3.79 (s, 3H), 3.74 (s, 3H), 3.61 (s, 2H), 2.27 (s, 3H), 2.25 (s, 3H), 1.07 (m, 1H), 0.50 (m, 1H), 0.39 (m, 2H), 0.31 (m, 1H); ^{13}C NMR (DMSO-d_6, 75 MHz): δ 165.8, 162.7, 160.1, 152.5, 151.5, 146.1, 143.0, 140.8, 136.44, 136.41, 135.8, 130.4, 127.9, 127.5, 126.7, 121.6, 118.5, 118.2, 114.8, 106.6, 60.8, 55.8, 53.2, 32.2, 19.7, 19.1, 16.8, 3.8, 2.0. Anal. Calcd for $C_{29}H_{32}N_6O_3 \cdot 1.8\ H_2O$: C, 63.91; H, 6.58; N, 15.42. Found: C, 63.70; H, 6.19; N, 15.13.

*5.5.4. (±)-(E)-3-(5-((2,4-Diaminopyrimidin-5-yl)methyl)-2,3-dimethoxyphenyl)-1-(6,7-dimethyl-1-vinylphthalazin-2(1H)-yl)prop-2-en-1-one (**13d**):* This compound was prepared using the same procedure as above. Yield: 1.25 g (54%) as a white solid, mp 215-217 °C; IR: 3358, 3178, 3071, 1662, 1631, 1595 cm^{-1}; ^{1}H NMR (DMSO-d_6, 400

MHz): δ 7.87 (d, *J* = 16.1 Hz, 1H), 7.80 (s, 1H), 7.66 (d, *J* = 16.1 Hz, 1H), 7.58 (s, 1H), 7.27 (s, 2H), 7.24 (s, 1H), 7.01 (s, 1H), 6.65 (br s, 2H), 6.28 (d, *J* = 4.7 Hz, 1H), 6.23 (br s, 2H), 5.77 (ddd, *J* = 15.9, 10.2, 4.7 Hz, 1H), 5.04 (d, *J* = 10.1 Hz, 1H), 4.78 (d, *J* = 16.6 Hz, 1H), 3.80 (s, 3H), 3.75 (s, 3H), 3.61 (s, 2H), 2.28 (s, 3H), 2.26 (s, 3H); ^{13}C NMR (DMSO-d_6, 101 MHz): δ 164.9, 162.0, 159.6, 151.9, 151.1, 145.5, 141.5, 140.4, 136.13, 136.06, 135.3, 134.9, 128.7, 127.2, 127.1, 126.4, 120.7, 117.9, 117.3, 114.4, 114.3, 105.9, 60.2, 55.2, 51.7, 31.6, 19.1, 18.5. Anal. Calcd for $C_{28}H_{30}N_6O_3 \cdot 2.1\ H_2O$: C, 62.70; H, 6.43; N, 15.67. Found: C, 62.57; H, 6.09; N, 15.52.

*5.5.5. (±)-(E)-3-(5-((2,4-Diaminopyrimidin-5-yl)methyl)-2,3-dimethoxyphenyl)-1-(6,7-dimethyl-1-(2-methylprop-1-en-1-yl)phthalazin-2(1H)-yl)prop-2-en-1-one (**13e**):* This compound was prepared using the same procedure as above. Yield: 1.26 g (58%) as a yellow solid, mp 212-213 °C; IR: 3425, 3360, 3192, 1668, 1636, 1596 cm^{-1}; ^{1}H NMR (DMSO-d_6, 400 MHz): δ 7.84 (d, *J* = 16.1 Hz, 1H), 7.81 (s, 1H), 7.60 (s, 1H), 7.59 (d, *J* = 16.1 Hz, 1H), 7.24 (s, 1H), 7.23 (s, 1H), 7.05 (s, 1H), 6.99 (s, 1H), 6.40 (d, *J* = 9.8 Hz, 1H), 6.29 (br s, 2H), 5.84 (br s, 2H), 5.18 (d, *J* = 9.8 Hz, 1H), 3.79 (s, 3H), 3.74 (s, 3H), 3.60 (s, 2H), 2.25 (s, 3H), 2.23 (s, 3H), 1.96 (s, 3H), 1.59 (s, 3H); ^{13}C NMR (DMSO-d_6, 101 MHz): δ 165.2, 162.3, 161.8, 154.9, 152.5, 146.0, 142.1, 141.2, 136.5, 136.4, 136.3, 133.0, 131.5, 127.9, 127.0, 122.5, 120.9, 118.3, 118.0, 114.7, 105.9, 60.8, 55.7, 49.0, 32.4, 25.3, 19.6, 19.6, 18.4 (1 aromatic C was unresolved). Anal. Calcd for $C_{30}H_{34}N_6O_3 \cdot 1.0\ H_2O$: C, 66.16; H, 6.66; N, 15.43. Found: C, 66.12; H, 6.48; N, 15.38.

*5.5.6. (±)-(E)-3-(5-((2,4-Diaminopyrimidin-5-yl)methyl)-2,3-dimethoxyphenyl)-1-(6,7-dimethyl-1-phenylphthalazin-2(1H)-yl)prop-2-en-1-one (**13f**):* This compound was prepared using the same procedure as above. Yield: 1.17 g (55%) as a white solid, mp 190-192 °C; IR: 3425, 3385, 3178, 1650, 1638, 1607, 1595 cm^{-1}; ^{1}H NMR (DMSO-d_6, 400 MHz): δ 7.88 (s, 1H), 7.85 (d, *J* = 16.1 Hz, 1H), 7.69 (d, *J* = 16.1 Hz, 1H), 7.58 (s, 1H), 7.35-7.17 (complex, 8H), 7.00 (s, 1H), 6.87 (s, 1H), 6.51 (br s, 2H), 6.04 (br s, 2H), 3.79 (s, 3H), 3.72 (s, 3H), 3.60 (s, 2H), 2.25 (s, 3H), 2.24 (s, 3H); ^{13}C NMR (DMSO-d_6, 101 MHz): δ 165.7, 162.5, 160.8, 152.9, 152.5, 146.1, 142.1, 142.0, 141.4, 136.9, 136.7, 136.1, 130.6, 128.6, 128.0, 127.7, 127.4, 127.1, 126.1, 120.8, 118.5, 117.8, 114.9, 106.3, 60.8, 55.7, 53.7, 32.2, 19.7, 19.0. Anal. Calcd for $C_{32}H_{32}N_6O_3 \cdot 3.5\ H_2O$: C, 62.83; H, 6.43; N, 13.74. Found: C, 62.72; H, 6.19; N, 13.56.

5.6 Assessment of inhibition

Measurements of the whole cell inhibition (MIC) and the enzymatic inhibition (K_i) utilized a racemic mixture of each inhibitor and followed previously published procedures [6, 30].

In brief, MIC values were based on standardized cultures of *S. aureus* strain 29213 as prescribed by the CLSI [40]. Evaluation of growth utilized spectrophotometric values of turbidity at 600 nm and on visual inspection for assessment of bacterial growth. The lowest concentration that yielded no growth after 18 h incubation was assigned as the MIC.

Evaluation of the enzymatic activity and inhibition utilized purified DHFR protein previously cloned from *S. aureus* and expressed recombinantly in *E. coli* BL21 (DE3) cells. The enzymatic reaction was reconstituted, including the NADPH co-factor and varied concentrations of inhibitor diluted from a 10 mM stock in DMSO, with initiation of the reaction by addition of the dihydrofolate substrate. The reaction was carried out at 30 ^{o}C and monitored for 2.8 min, during which time the rate was linear. These rates were plotted as a function of inhibitor concentration, and the 50% activity point was calculated using a 4-parameter curve fit (Prism 6.0d). The IC_{50} values were converted to K_i values using the Cheng-Prusoff equation and the previously measured K_M value [6, 41].

5.7 Crystallization and structure determination

Methods closely followed previously published procedures [6, 30]. The 6×His affinity tag was removed by digestion with thrombin, further purified using size exclusion chromatography, and concentrated to 12-15 mg/mL for crystallization. Solid racemic compound was added to saturation directly to the protein solution, followed by NADPH at a final concentration of 1 mM. After 2 h of incubation at room temperature, samples were centrifuged to remove excess saturated inhibitor and subjected to crystallization. Hanging drop vapor diffusion was carried out using 2 µL of protein solutions mixed with 2 µL of well solution containing 0.1 MES, pH 6.2-6.4, 0.1-0.2 M sodium acetate, and 18-25% polyethylene glycol 6000. Crystals typically grew to usable sizes within 1 week when incubated at room temperature.

Data were collected from crystals cryoprotected with 15% glycerol in mother liquor and saturated with inhibitor. Data collection was carried out at the University of Oklahoma

Macromolecular Crystallography Laboratory using a Rigaku RU3HR generator coupled with a Raxis 4^{++} image plate detector, or a Rigaku MicroMax 007HF generator coupled with a Dectris Pilatus 200K silicon pixel detector. Data from the Raxis 4^{++} detector were indexed and scaled using d*TREK v 9.7 [42], while those from the Dectris Pilatus were indexed and scaled using HKL3000 [43]. All structures were solved by molecular substitution with PDB ID 3M08 [6]. Refinement and rebuilding of the structures were carried out using the programs Phenix and Coot [44, 45].

Conflicts of Interest

The authors declare no competing interests.

Author Contributions

Chemical synthesis and analyses were carried out in the Chemistry Department at Oklahoma State University by N.P.M., B.N., R.A.B, and K.D.B. Remaining studies were carried out in the Chemistry and Biochemistry Department at the University of Oklahoma. Protein purification and crystallization was carried out by J.C.W. and C.R.B.; structure solution and analysis was carried out by J.C.W., L.M.T. and C.R.B. MIC determinations were made by C.R.B., and enzyme inhibition was measured by I.P. and C.R.B. All authors have approved the submitted form of this manuscript.

Acknowledgments

We gratefully acknowledge support of this work with start-up funds from the University of Oklahoma to C.R.B, and in the early stages from the National Institutes of Allergy and Infectious Diseases (R01-AI090685). The chemical syntheses were enabled by funding from NSF (BIR-9512269), the Oklahoma State Regents for Higher Education, the W. M. Keck Foundation, and Conoco, Inc., which included funding for a 300 MHz NMR spectrometer of the Oklahoma Statewide shared NMR facility. The authors also wish to thank the OSU College of Arts and Sciences for funds to purchase new FT-IR instruments and a new 400 MHz NMR spectrometer in the Chemistry Department. The OU Biomolecular Structure Core is supported in part by an Institutional Development Award (IDeA) from the National Institute of General Medical Sciences of the National

Institutes of Health (Award P20GM103640), the National Science Foundation (Award 0922269), and the University of Oklahoma Department of Chemistry and Biochemistry. Funders had no involvement in the study design, collection, analysis and interpretation, or writing of this report.

References

[1] E. Martens, A.L. Demain, The antibiotic resistance crisis, with a focus on the United States, J Antibiot (Tokyo), 70 (2017) 520-526.
[2] A. Cassini, L.D. Hogberg, D. Plachouras, A. Quattrocchi, A. Hoxha, G.S. Simonsen, M. Colomb-Cotinat, M.E. Kretzschmar, B. Devleesschauwer, M. Cecchini, D.A. Ouakrim, T.C. Oliveira, M.J. Struelens, C. Suetens, D.L. Monnet, Attributable deaths and disability-adjusted life-years caused by infections with antibiotic-resistant bacteria in the EU and the European Economic Area in 2015: a population-level modelling analysis, Lancet Infect Dis, 19 (2019) 56-66.
[3] R. Cave, R. Misra, J. Chen, S. Wang, H.V. Mkrtchyan, Whole genome sequencing revealed new molecular characteristics in multidrug resistant *Staphylococci* recovered from high frequency touched surfaces in London, Scientific reports, 9 (2019) 9637.
[4] Center for Disease Control, Vital Signs: Deadly Staph infections still threaten the U.S., in: Morbidity and Mortality Weekly Report, Centers for Disease Control, Atlanta, 2019.
[5] B. Srinivasan, S. Tonddast-Navaei, A. Roy, H. Zhou, J. Skolnick, Chemical space of *Escherichia coli* dihydrofolate reductase inhibitors: New approaches for discovering novel drugs for old bugs, Med Res Rev, 39 (2019) 684-705.
[6] C.R. Bourne, E.W. Barrow, R.A. Bunce, P.C. Bourne, K.D. Berlin, W.W. Barrow, Inhibition of antibiotic-resistant *Staphylococcus aureus* by the broad-spectrum dihydrofolate reductase inhibitor RAB1, Antimicrob Agents Chemother, 54 (2010) 3825-3833.
[7] K.M. Frey, M.N. Lombardo, D.L. Wright, A.C. Anderson, Towards the understanding of resistance mechanisms in clinically isolated trimethoprim-resistant, methicillin-resistant *Staphylococcus aureus* dihydrofolate reductase, J Struct Biol, 170 (2010) 93-97.
[8] C.P. Vicetti Miguel, A. Mejias, A. Leber, P.J. Sanchez, A decade of antimicrobial resistance in *Staphylococcus aureus*: A single center experience, PLoS One, 14 (2019) e0212029.
[9] S.M. Reeve, E.W. Scocchera, G.D. N, S. Keshipeddy, J. Krucinska, B. Hajian, J. Ferreira, M. Nailor, J. Aeschlimann, D.L. Wright, A.C. Anderson, MRSA Isolates from United States Hospitals Carry *dfrG* and *dfrK* Resistance Genes and Succumb to Propargyl-Linked Antifolates, Cell Chem Biol, 23 (2016) 1458-1467.
[10] Y. Minato, S. Dawadi, S.L. Kordus, A. Sivanandam, C.C. Aldrich, A.D. Baughn, Mutual potentiation drives synergy between trimethoprim and sulfamethoxazole, Nat Commun, 9 (2018) 1003.
[11] C.R. Bourne, Utility of the biosynthetic folate pathway for targets in antimicrobial discovery, Antibiotics, 3 (2014) 1-28.

[12] S.L. Kordus, A.D. Baughn, Revitalizing antifolates through understanding mechanisms that govern susceptibility and resistance, Medchemcomm, 10 (2019) 880-895.
[13] V. Francesconi, L. Giovannini, M. Santucci, E. Cichero, M.P. Costi, L. Naesens, F. Giordanetto, M. Tonelli, Synthesis, biological evaluation and molecular modeling of novel azaspiro dihydrotriazines as influenza virus inhibitors targeting the host factor dihydrofolate reductase (DHFR), Eur J Med Chem, 155 (2018) 229-243.
[14] M. Tonelli, L. Naesens, S. Gazzarrini, M. Santucci, E. Cichero, B. Tasso, A. Moroni, M.P. Costi, R. Loddo, Host dihydrofolate reductase (DHFR)-directed cycloguanil analogues endowed with activity against influenza virus and respiratory syncytial virus, Eur J Med Chem, 135 (2017) 467-478.
[15] C. Tian, M. Wang, Z. Han, F. Fang, Z. Zhang, X. Wang, J. Liu, Design, synthesis and biological evaluation of novel 6-substituted pyrrolo [3,2-d] pyrimidine analogues as antifolate antitumor agents, Eur J Med Chem, 138 (2017) 630-643.
[16] D. Fernandez-Villa, M.R. Aguilar, L. Rojo, Folic Acid Antagonists: Antimicrobial and Immunomodulating Mechanisms and Applications, Int J Mol Sci, 20 (2019).
[17] A. Wrobel, K. Arciszewska, D. Maliszewski, D. Drozdowska, Trimethoprim and other nonclassical antifolates an excellent template for searching modifications of dihydrofolate reductase enzyme inhibitors, J Antibiotics, 73 (2020) 5-27.
[18] The Pew Charitable Trusts, Antibiotics currently in global clinical development, 2019.
[19] D.B. Huang, M. Dryden, Iclaprim, a dihydrofolate reductase inhibitor antibiotic in Phase III of clinical development: a review of its pharmacology, microbiology and clinical efficacy and safety, Future Microbiol, 13 (2018) 957-969.
[20] M. Kurosu, S. Siricilla, K. Mitachi, Advances in MRSA drug discovery: where are we and where do we need to be?, Expert Opin Drug Discov, 8 (2013) 1095-1116.
[21] K. Smith, L.M. Ednie, P.C. Appelbaum, S. Hawser, S. Lociuro, Antistreptococcal activity of AR-709 compared to that of other agents, Antimicrob Agents Chemother, 52 (2008) 2279-2282.
[22] W.T. Jansen, A. Verel, J. Verhoef, D. Milatovic, In vitro activity of AR-709 against *Streptococcus pneumoniae*, Antimicrob Agents Chemother, 52 (2008) 1182-1183.
[23] E.E. Wyatt, W.R. Galloway, G.L. Thomas, M. Welch, O. Loiseleur, A.T. Plowright, D.R. Spring, Identification of an anti-MRSA dihydrofolate reductase inhibitor from a diversity-oriented synthesis, Chem Commun (Camb), (2008) 4962-4964.
[24] S.M. Reeve, E. Scocchera, J.J. Ferreira, G.D. N, S. Keshipeddy, D.L. Wright, A.C. Anderson, Charged propargyl-linked antifolates reveal mechanisms of antifolate resistance and Inhibit trimethoprim-resistant MRSA strains possessing clinically relevant mutations, J Med Chem, 59 (2016) 6493-6500.
[25] C.R. Bourne, R.A. Bunce, P.C. Bourne, K.D. Berlin, E.W. Barrow, W.W. Barrow, Crystal structure of *Bacillus anthracis* dihydrofolate reductase with the dihydrophthalazine-based trimethoprim derivative RAB1 provides a structural explanation of potency and selectivity, Antimicrob Agents Chemother, 53 (2009) 3065-3073.
[26] C.R. Bourne, N. Wakeham, N. Webb, B. Nammalwar, R.A. Bunce, K.D. Berlin, W.W. Barrow, The structure and competitive substrate inhibition of dihydrofolate

reductase from *Enterococcus faecalis* reveal restrictions to cofactor docking, Biochemistry, 53 (2014) 1228-1238.
[27] B. Nammalwar, R.A. Bunce, K.D. Berlin, C.R. Bourne, P.C. Bourne, E.W. Barrow, W.W. Barrow, Synthesis and biological activity of substituted 2,4-diaminopyrimidines that inhibit *Bacillus anthracis*, Eur J Med Chem, 54 (2012) 387-396.
[28] B. Nammalwar, R.A. Bunce, K.D. Berlin, C.R. Bourne, P.C. Bourne, E.W. Barrow, W.W. Barrow, Microwave-assisted Heck synthesis of substituted 2,4-Diaminopyrimidine-based antibiotics, Org Prep Proced Int, 44 (2012) 281-287.
[29] N.P. Muddala, B. Nammalwar, S. Selvaraju, C.R. Bourne, M. Henry, R.A. Bunce, K.D. Berlin, E.W. Barrow, W.W. Barrow, Evaluation of New Dihydrophthalazine-Appended 2,4-Diaminopyrimidines against Bacillus anthracis: Improved Syntheses Using a New Pincer Complex, Molecules, 20 (2015) 7222-7244.
[30] B. Nammalwar, C.R. Bourne, R.A. Bunce, N. Wakeham, P.C. Bourne, K. Ramnarayan, S. Mylvaganam, K.D. Berlin, E.W. Barrow, W.W. Barrow, Inhibition of Bacterial Dihydrofolate Reductase by 6-Alkyl-2,4-diaminopyrimidines, ChemMedChem, 7 (2012) 1974-1982.
[31] B. Nammalwar, C.R. Bourne, N. Wakeham, P.C. Bourne, E.W. Barrow, N.P. Muddala, R.A. Bunce, K.D. Berlin, W.W. Barrow, Modified 2,4-diaminopyrimidine-based dihydrofolate reductase inhibitors as potential drug scaffolds against *Bacillus anthracis*, Bioorg Med Chem, 23 (2015) 203-211.
[32] H. Heaslet, M. Harris, K. Fahnoe, R. Sarver, H. Putz, J. Chang, C. Subramanyam, G. Barreiro, J.R. Miller, Structural comparison of chromosomal and exogenous dihydrofolate reductase from *Staphylococcus aureus* in complex with the potent inhibitor trimethoprim, Proteins, 76 (2009) 706-717.
[33] J.F. Darby, A.P. Hopkins, S. Shimizu, S.M. Roberts, J.A. Brannigan, J.P. Turkenburg, G.H. Thomas, R.E. Hubbard, M. Fischer, Water networks can determine the affinity of ligand binding to proteins, J Am Chem Soc, 141 (2019) 15818-15826.
[34] H. Cao, J. Skolnick, Time-resolved x-ray crystallography capture of a slow reaction tetrahydrofolate intermediate, Struct Dyn, 6 (2019) 024701.
[35] W.F. Holcomb, C.S. Hamilton, Derivatives of 4-amino-6-methoxyquinaldine, J Am Chem Soc, 64 (1942) 1309-1311.
[36] F.C. Whitmore, H. Mosher, R.R. Adams, R.B. Taylor, E.C. Chapin, C. Weisel, W. Yanko, Basically substituted aliphatic nitriles and their catalytic reduction to amines, J. Am. Chem. Soc., 66 (1944) 725-731.
[37] S. Nimgirawath, Synthesis of (±)-isoautumnaline and (±)-dysoxyline, Aust. J. Chem., 47 (1994) 957-962.
[38] A. Stuart, T. Paterson, B. Roth, E. Aig, 2,4-Diamino-5-benzylpyrimidines and analogues as antibacterial agents. 6. A one-step synthesis of new trimethoprim derivatives and activity analysis by molecular modeling, J. Med. Chem., 26 (1983) 667-673.
[39] R.A. Bunce, R. Harrison, B. Nammalwar, Efficient synthesis of selected phthalazine derivatives, Hetrocycl Commun, 18 (2012) 123-126.
[40] CLSI, Methods for dilution antimicrobial susceptibility tests for bacteria that grow aerobically; approved standard 8th edition, 29 (2009) 1-65.

[41] Y. Cheng, W.H. Prusoff, Relationship between the inhibition constant (Ki) and the concentration of inhibitor which causes 50 per cent inhibition (I50) of an enzymatic reaction, Biochem Pharmacol, 22 (1973) 3099-3108.
[42] J.W. Pflugrath, The finer things in X-ray diffraction data collection, Acta Crystallogr D Biol Crystallogr, 55 (1999) 1718-1725.
[43] W. Minor, M. Cymborowski, Z. Otwinowski, M. Chruszcz, HKL-3000: the integration of data reduction and structure solution--from diffraction images to an initial model in minutes, Acta Crystallogr D Biol Crystallogr, 62 (2006) 859-866.
[44] P.D. Adams, P.V. Afonine, G. Bunkoczi, V.B. Chen, I.W. Davis, N. Echols, J.J. Headd, L.W. Hung, G.J. Kapral, R.W. Grosse-Kunstleve, A.J. McCoy, N.W. Moriarty, R. Oeffner, R.J. Read, D.C. Richardson, J.S. Richardson, T.C. Terwilliger, P.H. Zwart, PHENIX: a comprehensive Python-based system for macromolecular structure solution, Acta crystallographica. Section D, Biological crystallography, 66 (2010) 213-221.
[45] P. Emsley, B. Lohkamp, W.G. Scott, K. Cowtan, Features and development of Coot, Acta crystallographica, 66 (2010) 486-501.

Figure Legends

Figure 1. The scaffold for this inhibitor series was varied with respect to the substituent at the chiral R_3 position, as well as modifications at the edge of the dihydrophthalazine heterocycle at $R_1 = R_2$. Racemic mixtures (at R_3) were tested for *in vitro* DHFR inhibition (K_i, blue bars with SEM, $n \geq 3$ independent assays with duplicate technical replicates) and for their ability to block growth of *S. aureus* cultures (MIC, red bars with SEM, $n = 2$ independent assays with duplicate technical replicates). Numerical values are given in the Supplemental Material.

Figure 2. Inhibitors displace a conserved water network and fit into the folate pocket through shape complementarity. A. DAP moieties mimic the native water network in the folate pocket. **B.** The predominant interactions between DHFR and the scaffold are hydrophobic (electrostatic surface is displayed). **C.** The R_3 modifications are observed as *S*-enantiomers and occupy a conserved hydrophobic region (surface colored green for polar, orange for hydrophobic).

Figure 3. Appending methoxy moieties at the distal edge of the dihydrophthalazine scaffold creates a strained fit within the folate pocket. A. This strain is tolerated when a larger hydrophobic group is at R_3, although the dihydrophthalazine heterocycle is shifted approx. 0.7 Å higher in the site. **B.** A smaller R_3 group (cyclopropyl) does not impose the same energetic cost for solvent exposure, allowing relief of the strain at the phthalazine by rotating the distal inhibitor scaffold into an alternate binding ledge unique to SaDHFR.

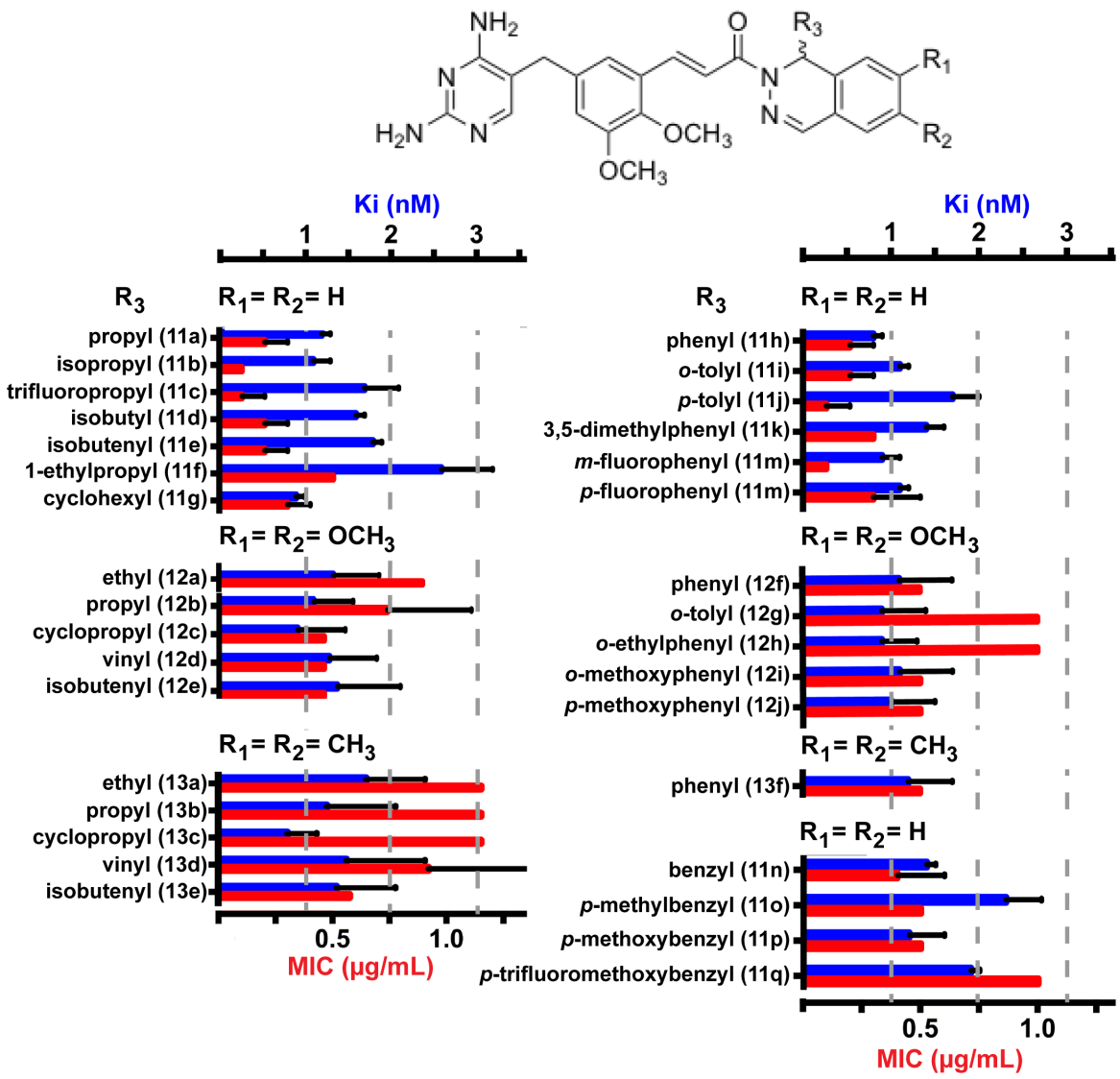
NH2
O
R3
R1
N
N
N
H2N
N
OCH3
R2
OCH3
Ki (nM)
1
2
3
R3
R1= R2= H
propyl (11a)
isopropyl (11b)
trifluoropropyl (11c)
isobutyl (11d)
isobutenyl (11e)
1-ethylpropyl (11f)
cyclohexyl (11g)
R1= R2= OCH3
ethyl (12a)
propyl (12b)
cyclopropyl (12c)
vinyl (12d)
isobutenyl (12e)
R1= R2= CH3
ethyl (13a)
propyl (13b)
cyclopropyl (13c)
vinyl (13d)
isobutenyl (13e)
0.5
1.0
MIC (μg/mL)
Ki (nM)
1
2
3
R3
R1= R2= H
phenyl (11h)
o-tolyl (11i)
p-tolyl (11j)
3,5-dimethylphenyl (11k)
m-fluorophenyl (11m)
p-fluorophenyl (11m)
R1= R2= OCH3
phenyl (12f)
o-tolyl (12g)
o-ethylphenyl (12h)
o-methoxyphenyl (12i)
p-methoxyphenyl (12j)
R1= R2= CH3
phenyl (13f)
R1= R2= H
benzyl (11n)
p-methylbenzyl (11o)
p-methoxybenzyl (11p)
p-trifluoromethoxybenzyl (11q)
0.5
1.0
MIC (μg/mL)

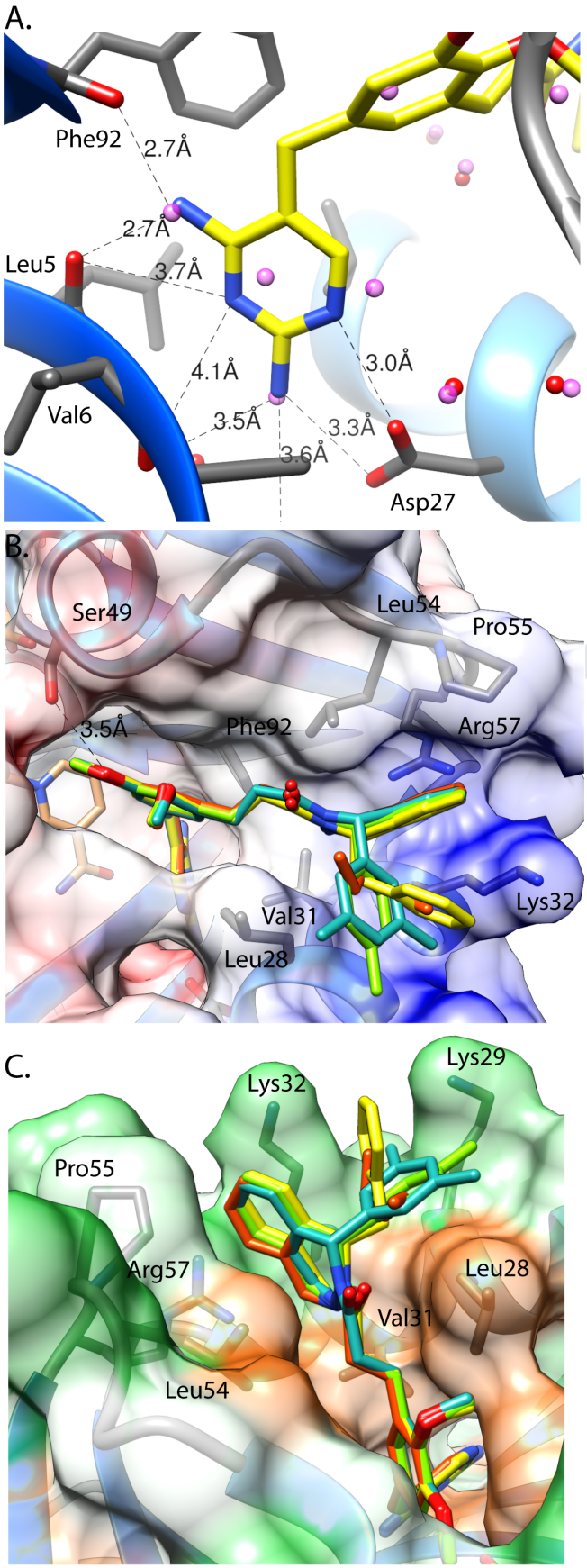
A.
Phe92
2.7Å
2.7Å
Leu5
3.7Å
4.1Å
3.0Å
Val6
3.5Å
3.3Å
3.6Å
Asp27
B.
Ser49
Leu54
Pro55
3.5Å
Phe92
Arg57
Lys32
Val31
Leu28
C.
Lys29
Lys32
Pro55
Arg57
Leu28
Val31
Leu54

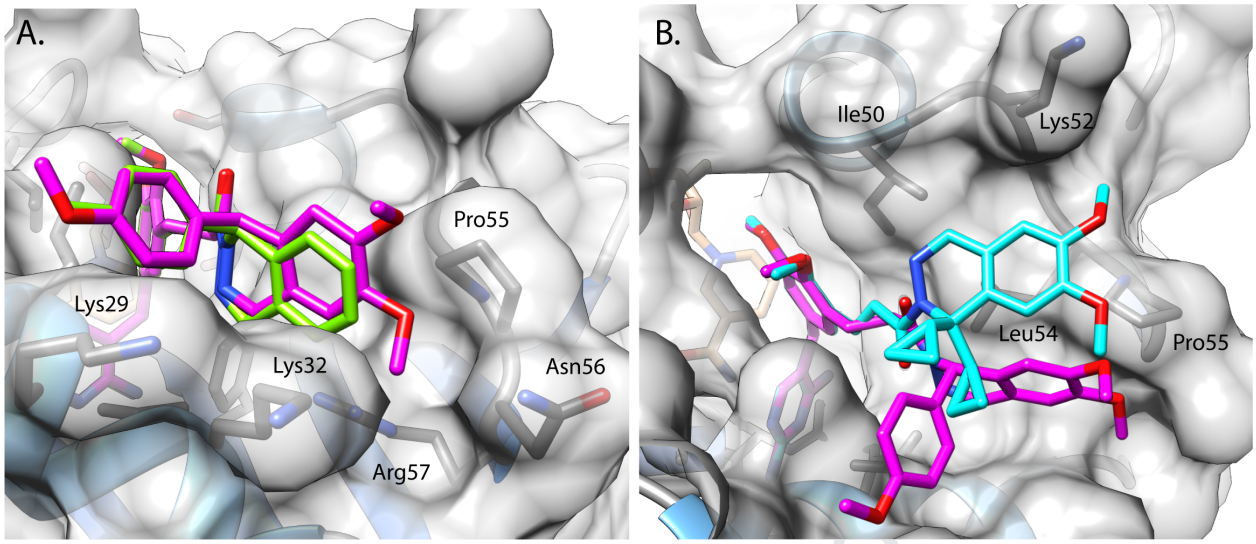

Highlights for "**Inhibitor design to target a unique feature in the folate pocket of *Staphylococcus aureus* dihydrofolate reductase"**

N. Prasad Muddala[1,¶,#a], John C. White[2,¶], Baskar Nammalwar[1,#b], Ian Pratt[2], Leonard M. Thomas[2], Richard A. Bunce[1], K. Darrell Berlin[1], and Christina R. Bourne[2*]

Trimethoprim derivatives offer additional chemical diversity within a proven scaffold

Antibiotic resistance development increases the need for new antibiotic derivatives

Altering chemical moieties at the binding site: solvent interface modulates affinity

Altering chemical moieties at the dihydrophthalazine edge alters cell inhibition

Combining moieties improves inhibition by targeting a unique binding site surface

Derivatives targeting this site do not prefer a specific enantiomer

Declaration of interests

☒ The authors declare that they have no known competing financial interests or personal relationships that could have appeared to influence the work reported in this paper.

☐The authors declare the following financial interests/personal relationships which may be considered as potential competing interests: